The Abdus Salam International Centre for Theoretical Physics

United Nations Educational, Scientific and Cultural Organization

IAEA International Atomic Energy Agency

2139-29

School on Synchrotron and Free-Electron-Laser Sources and their Multidisciplinary Applications

26 April - 7 May, 2010

Two-colour and photon correlation spectroscopy with lasers and FELs

Fulvio Parmigiani

University of Trieste
Trieste
ITALY

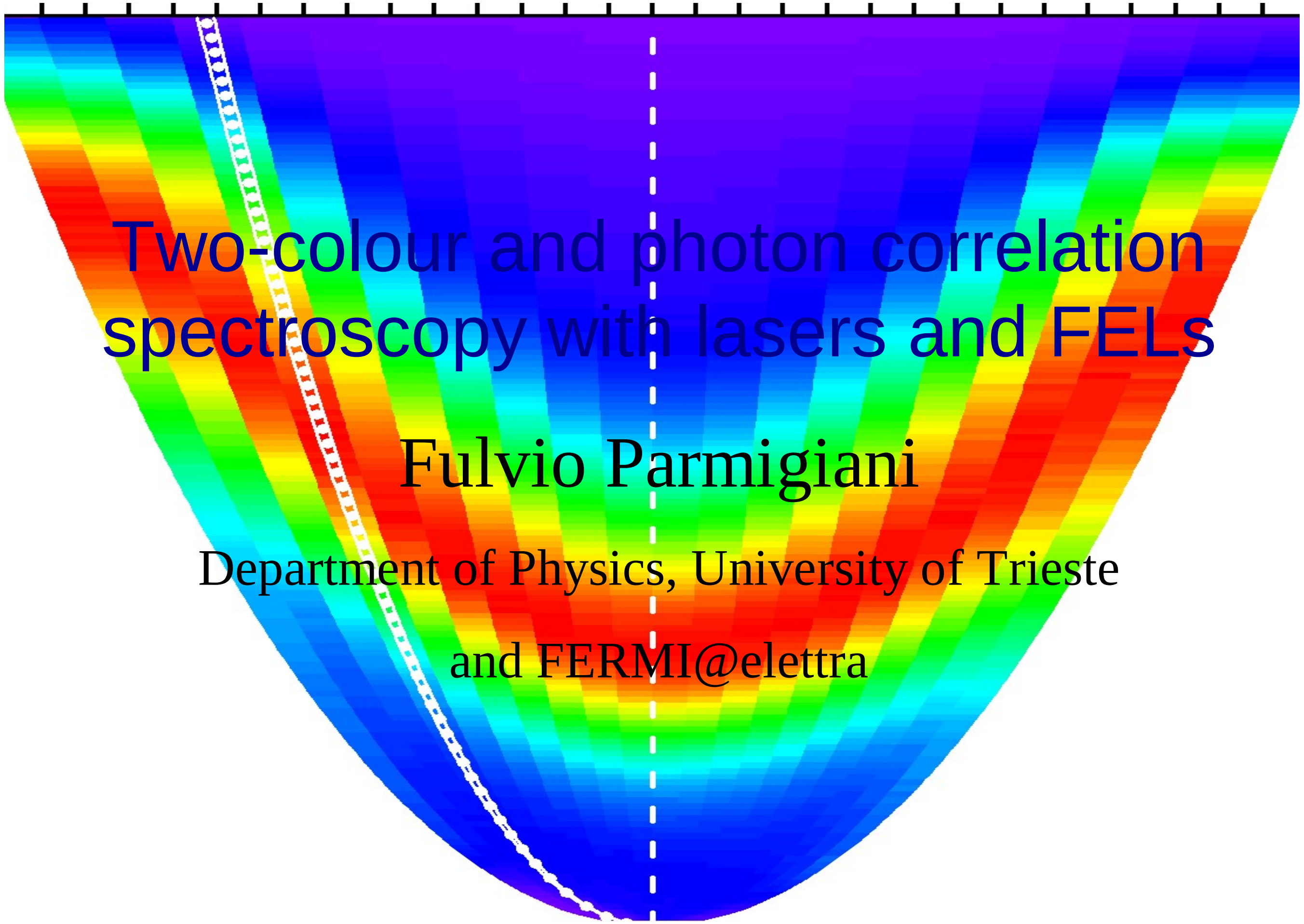

Two-colour and photon correlation spectroscopy with lasers and FELs

Fulvio Parmigiani

Department of Physics, University of Trieste

and FERMI@elettra

The study of the electron dynamics relays on the ability to time-resolve the ultra-rapid scattering processes which result in energy and momentum relaxation, recombination and diffusion.

In typical experiments a short-pulsed (10-100 fs) laser can be used for photoemission experiments in the time-domain, whereas longer laser pulses (1-5 ps) provided by FT limited coherent sources can be used for photoemission experiments in the frequency (energy) domain with unrecorded resolving power.

Experimental techniques must be brought to bear in which band-structure specificity are combined with time resolution. Angle resolved photoemission is particularly suited for such experiments.

A glance on the photoemission

A few new directions in photoemission measurements

Curtesy C. Fadley, UC Davis & ALS

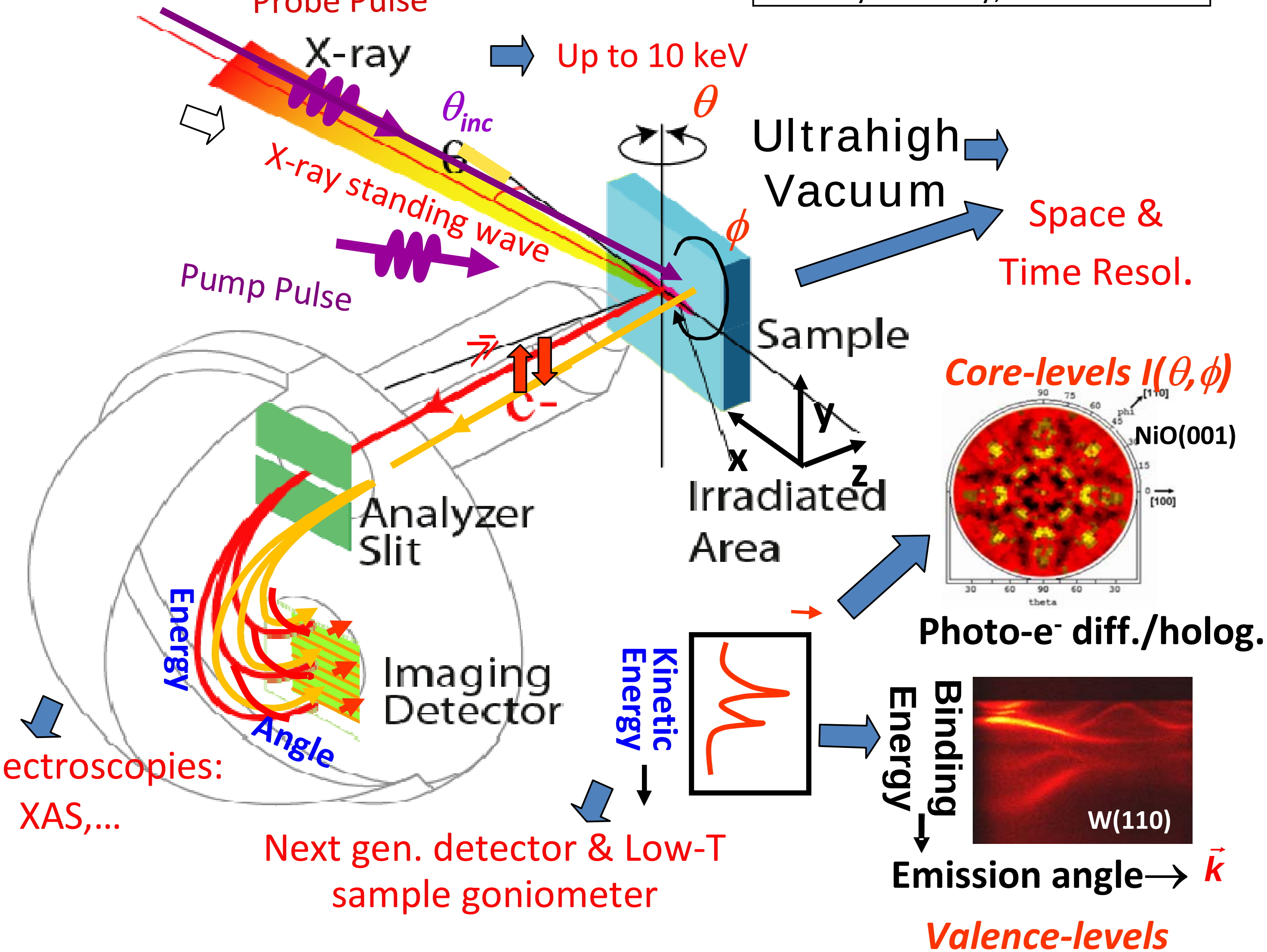

+ Other spectroscopies: XES, XAS,…

Next gen. detector & Low-T sample goniometer

LINEAR PHOTOEMISSION ($h\nu > \Phi$) ⟶

band mapping of OCCUPIED STATES

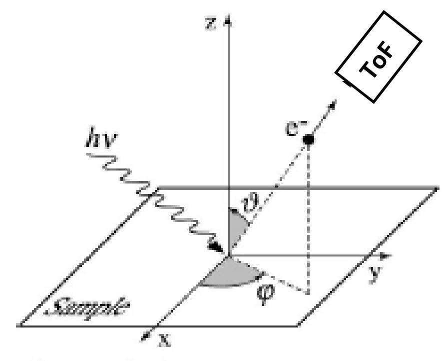

Photoemission geometry

$$E_{kin} = h\nu - E_B - \phi$$

$$k_{//} = \sqrt{2mE_{kin}/\hbar^2} \cdot \sin\theta$$

TIME RESOLVED MULTI-PHOTON PHOTOEMISSION ($h\nu < \Phi$) ⟶

band mapping of UNOCCUPIED STATES and ELECTRON SCATTERING PROCESSES mechanisms

Polarization Coherence and selection rules

Absorption Intensity ~ $| \langle f | \mathbf{D} | i \rangle |^2$

$\mathbf{D} = \mathbf{E} \bullet \mathbf{r}$ is dipole operator

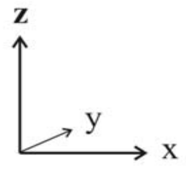

Linear

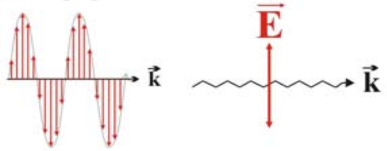

$D \sim z \sim r\ Y_1^0$

Right circular

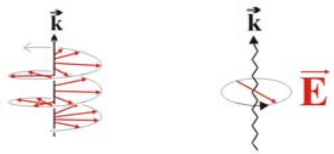

$D \sim x + i y \sim r Y_1^{+1}$

Left circular

$D \sim x - i y \sim r Y_1^{-1}$

Selection rules:

$\Delta l = \pm 1, \quad \Delta s = 0, \quad \Delta j = 0, \pm 1$

$$\Delta E \bullet \Delta t \geq \frac{h}{2}$$

$$i\hbar \frac{\partial}{\partial t}\Psi = -\frac{\hbar^2}{2m}\nabla^2\Psi + V\Psi$$

$$x(t) = \frac{1}{2\pi}\int_{-\infty}^{\infty} X(\omega)\, e^{i\omega t}\, d\omega, \quad X(\omega) = \int_{-\infty}^{\infty} x(t)\, e^{-i\omega t}\, dt$$

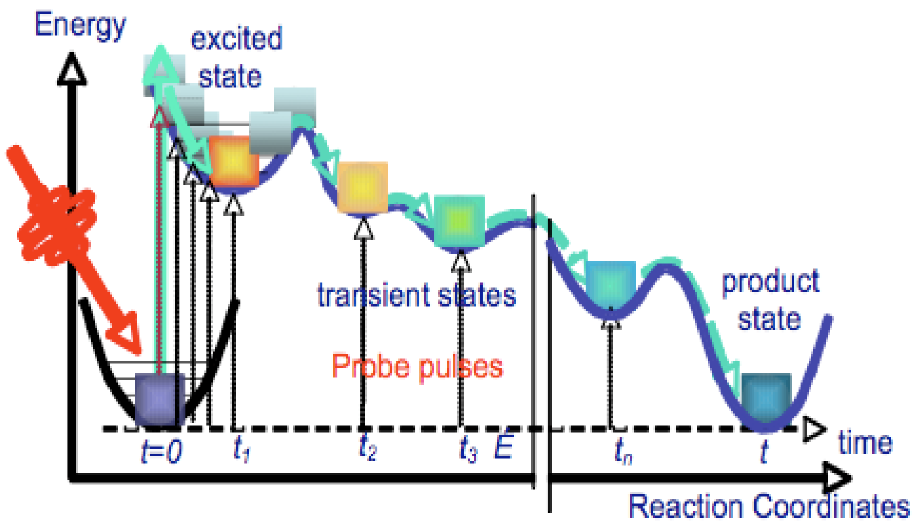

A fs molecular movie. A laser pulse excites the system, and then the resulting cascade of transient states is probed at various time intervals until the product state is formed (image courtesy of Lin Chen, Argonne).

Experimental Set-up

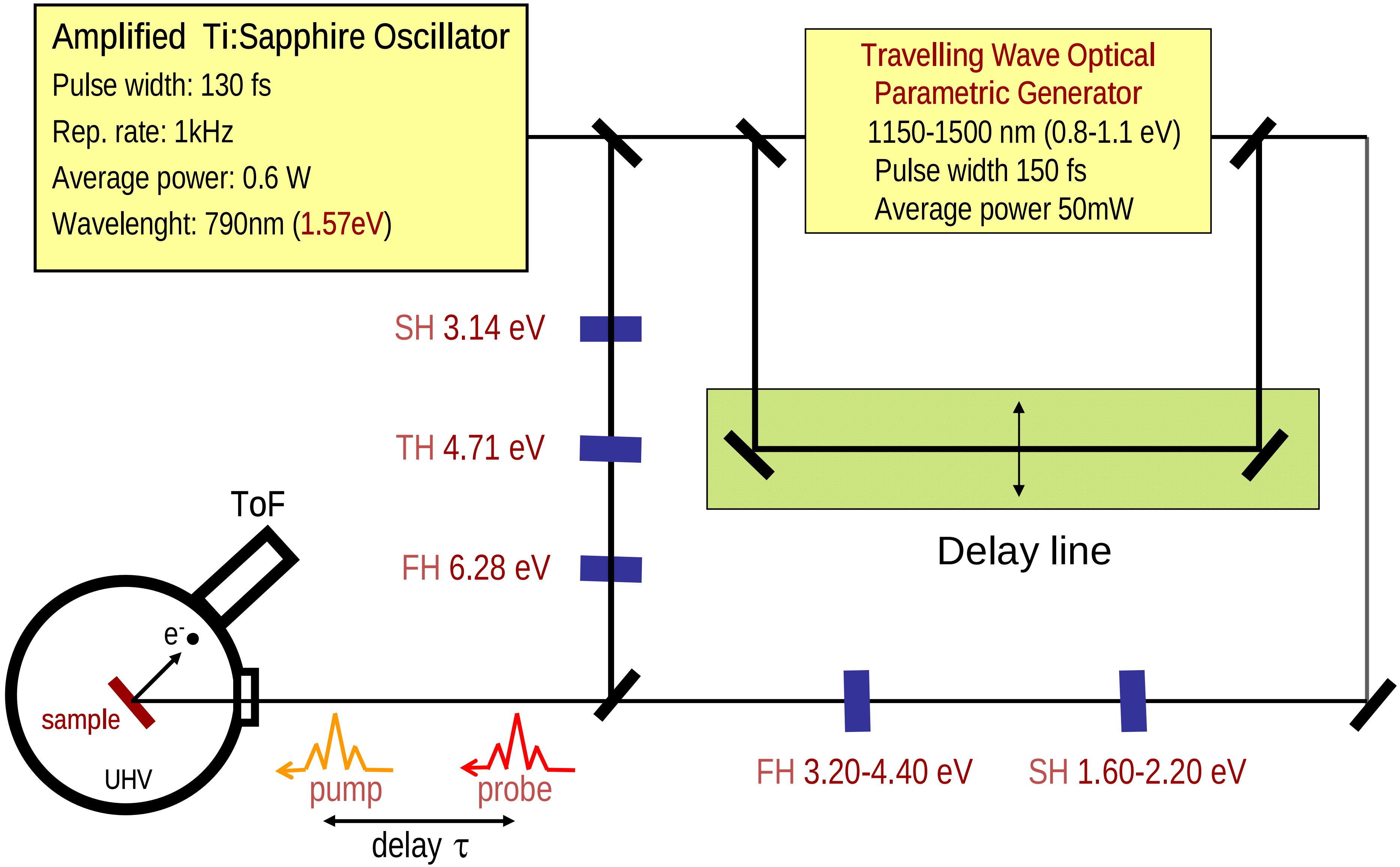

HGHG Free Electron Laser (FEL)

Ultra-fast laser pulse slicing of the synchrotron electron bunch

HHG in a hollow fiber yields a longer interaction length and "phase-matching."

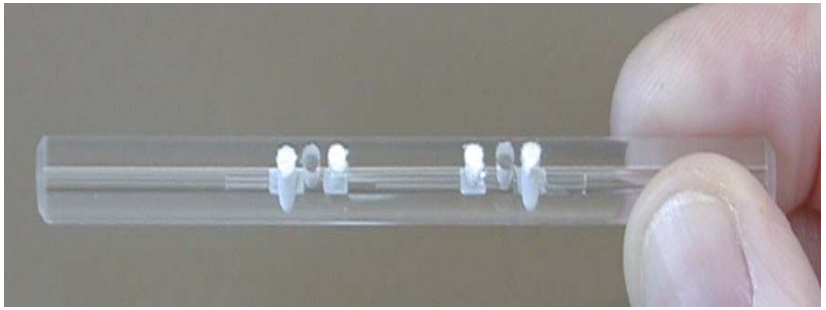

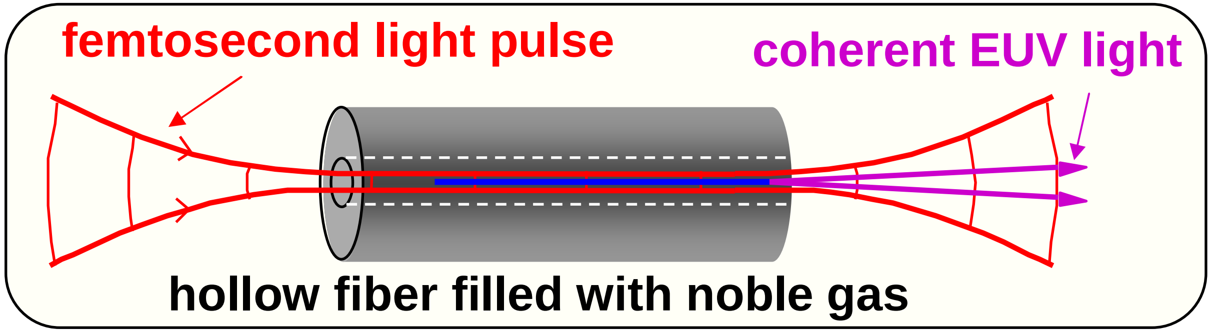

Science **280**, 1412 (1998)

High Harmonic Generation laser source

time

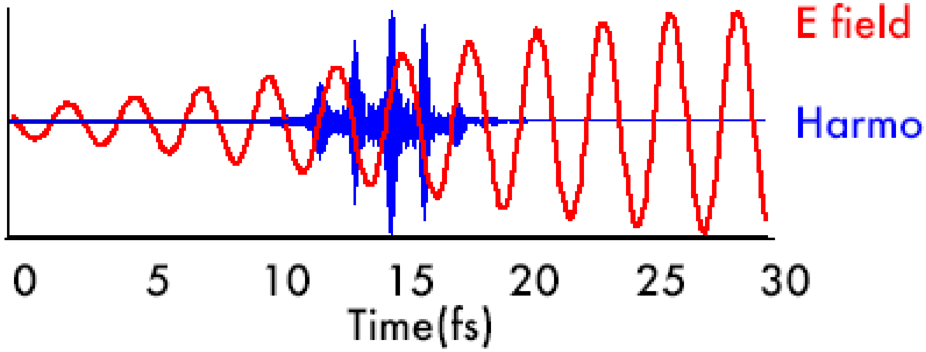

I. Christov et al, PRL 78, 1251, (1997)

frequency

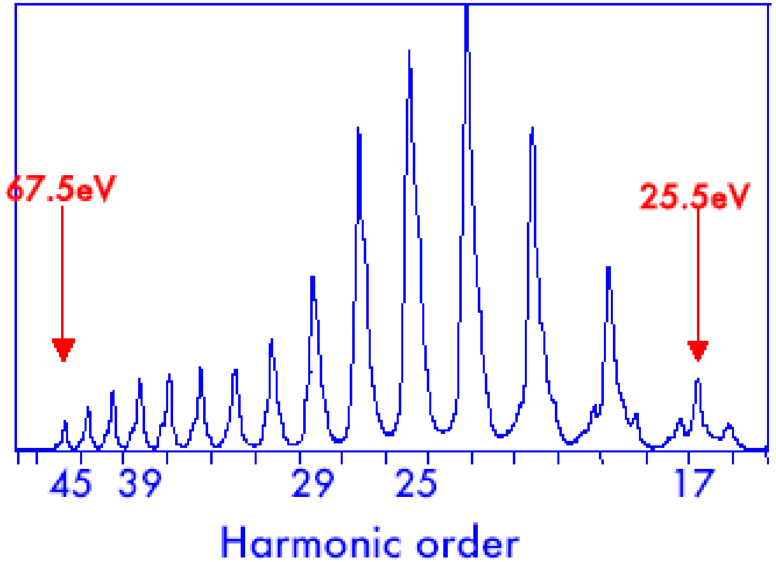

J. Zhou et al, PRL 76(5), 752-755 (1996)

FERMI System Layout

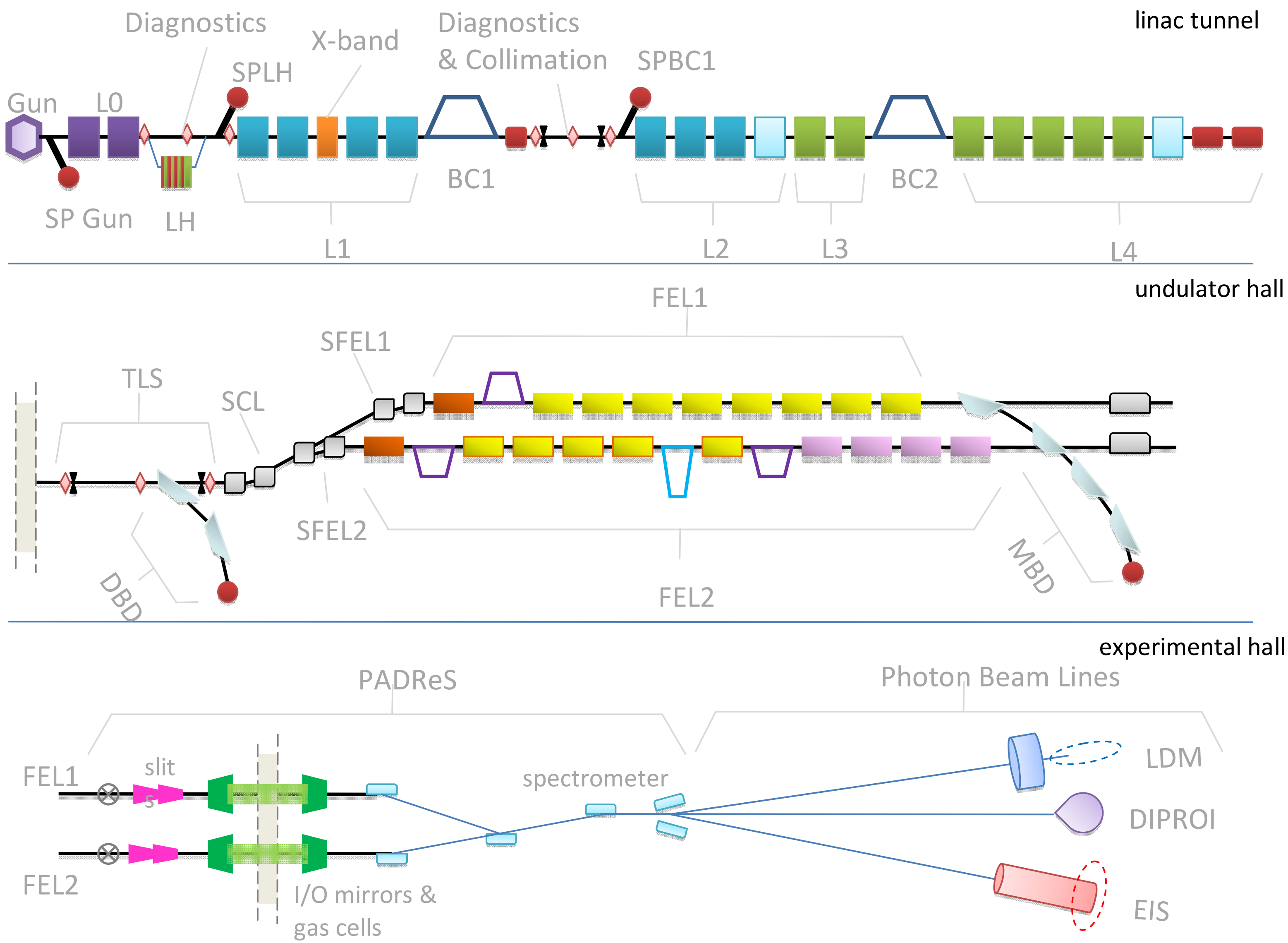

Experimental Set-up

- μ-metal UHV chamber
- residual magnetic field < 10 mG
- Base pressure $<2 \cdot 10^{-10}$ mbar
- photoemitted electrons detector:
  Time of Flight (ToF) spectrometer

Acceptance angle:
± 0.83°
Energy resolution:
10 meV @ 2eV
Detector noise:
$<10^{-4}$ counts/s

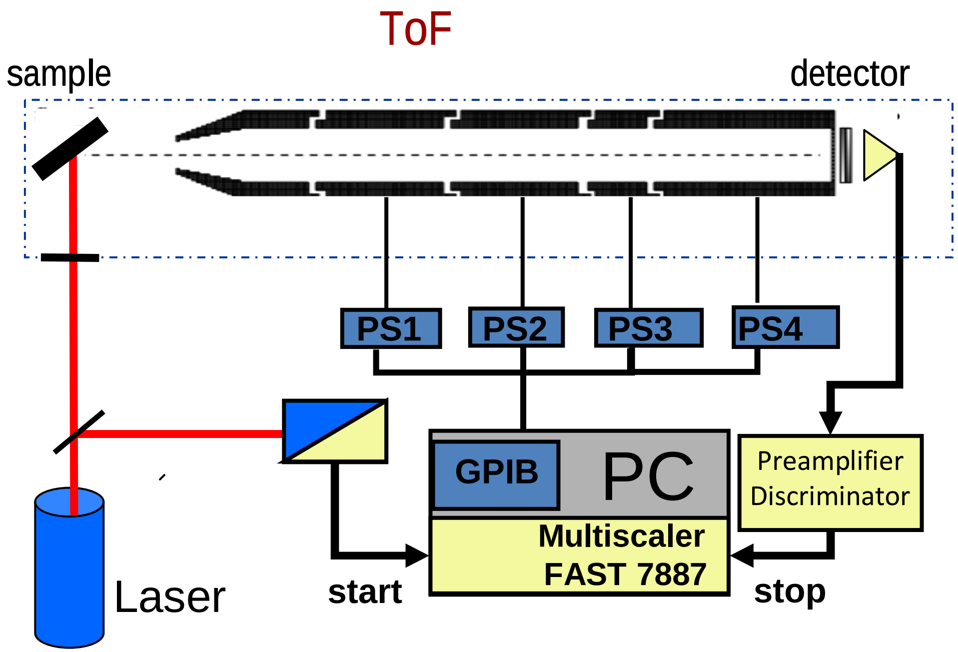

G. Paolicelli et al. Surf. Rev. and Lett. **9**, 541 (2002)

Experimental Set-up

Time-Resolved and Angle Resolved Photoelectron Spectroscopy – TR-ARPES and Time-Resolved and Spin Resolved ARPES – TR-SR-ARPES
(started 2006)

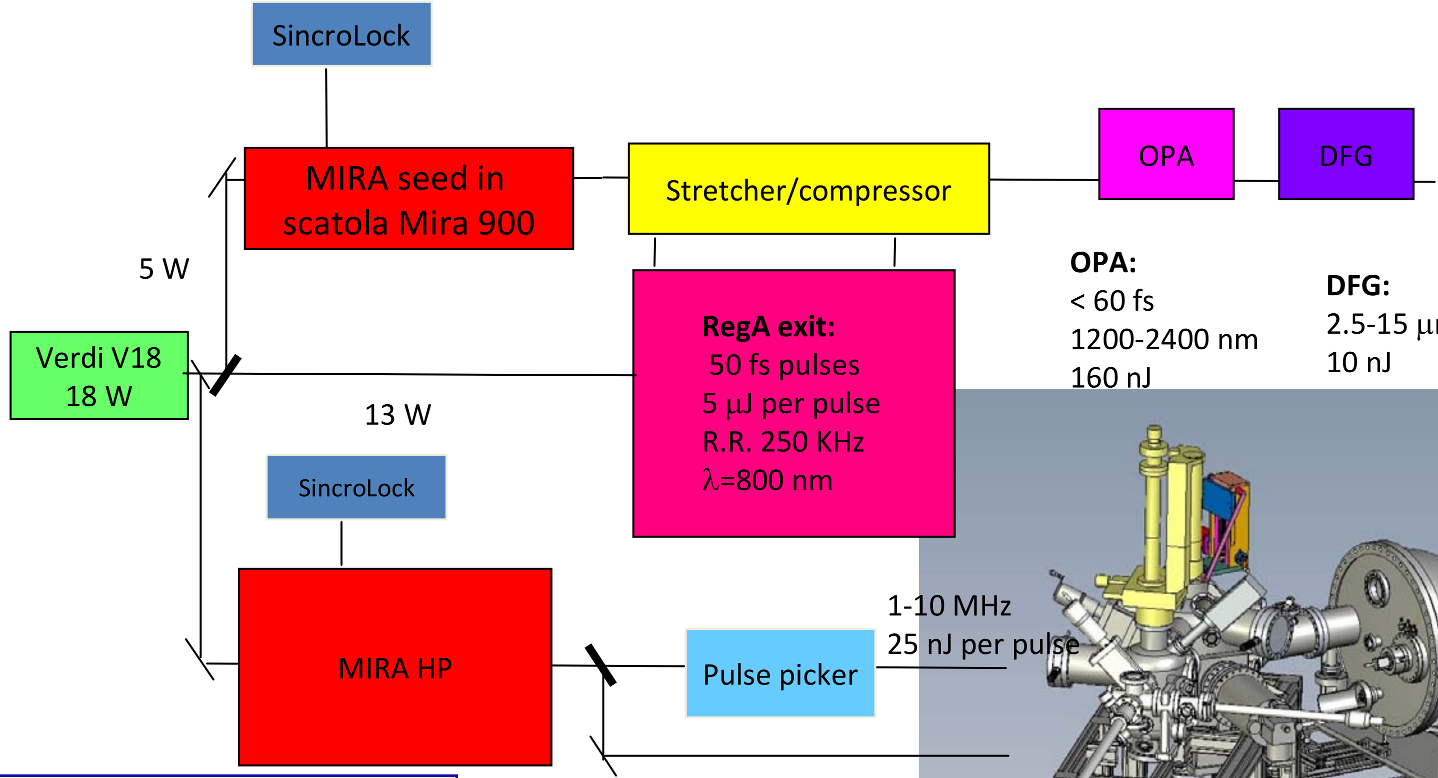

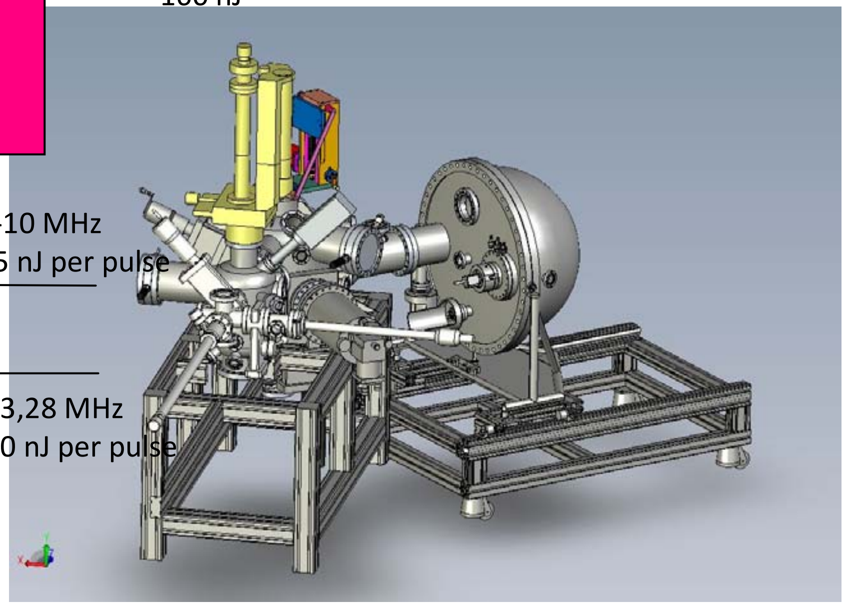

10 K Minimum Temperature on the Sample
6 degrees of Freedom motorized
sub meV Resolution
40 degrees Angular Acceptance
Max Ang Resolution 0.1 degrees
Plug and play upgradable for Spin detection

ToF-SPIN DETECTOR

Time-of-Flight analyser
@ high operating frequency
(up to 5 MHz)

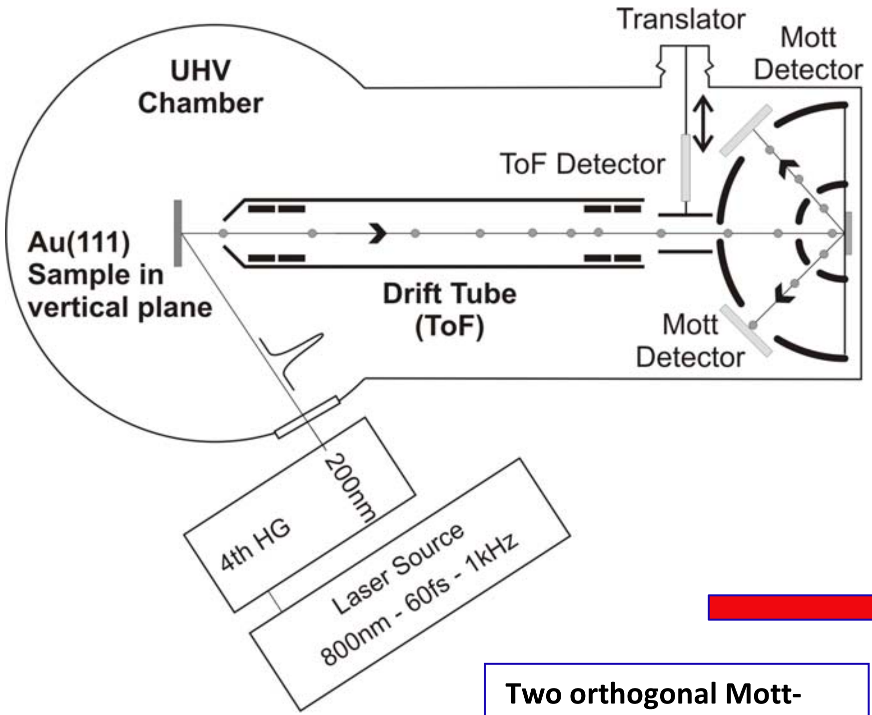

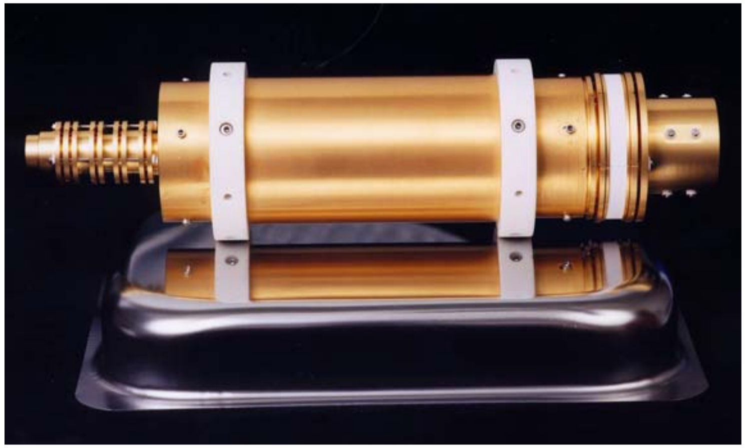

Two orthogonal Mott-detectors to measure V and H spin components

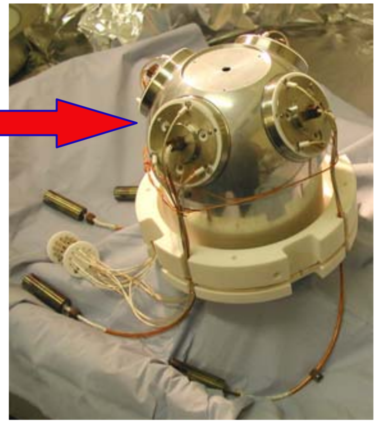

Electron detector

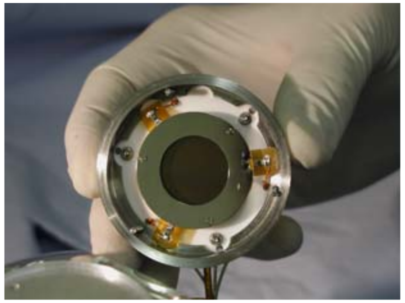

Mott polarimeter

Collaboration with 4GLS (E. Seddon and C. Cacho)

Photoemission Spectra on Ag(100) single crystal

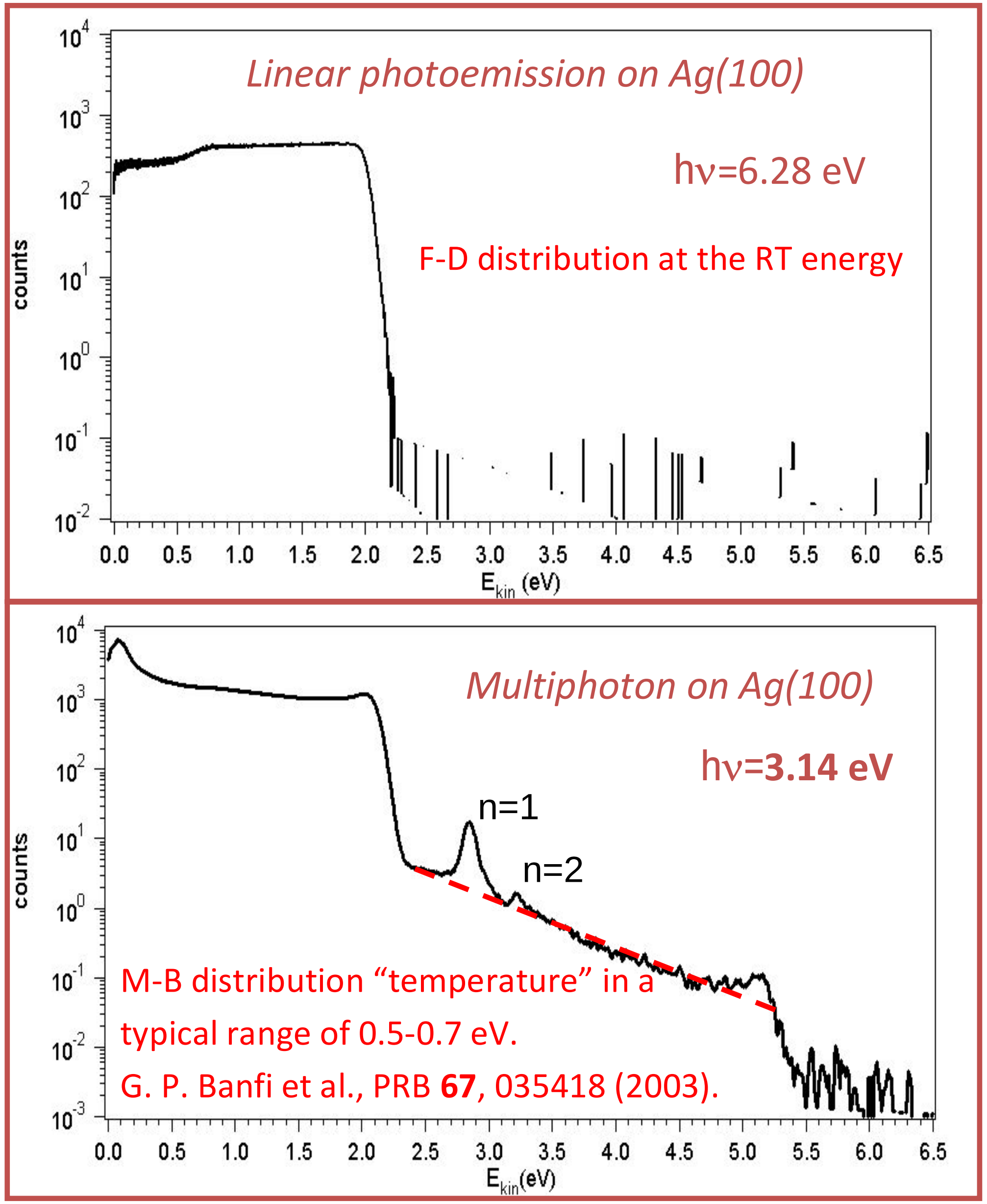

***p*-polarized incident radiation**
30° incidence and 150 fs pulse.

Log Scale
10^6 sensitivity

I_{abs}=13 mJ/cm^2

NON-LINEAR PHOTOEMISSION on METALS

and

NON-EQUILIBRIUM ELECTRON DYNAMICS

Time Resolved 2-Photon Photoemission (TR-2PPE)

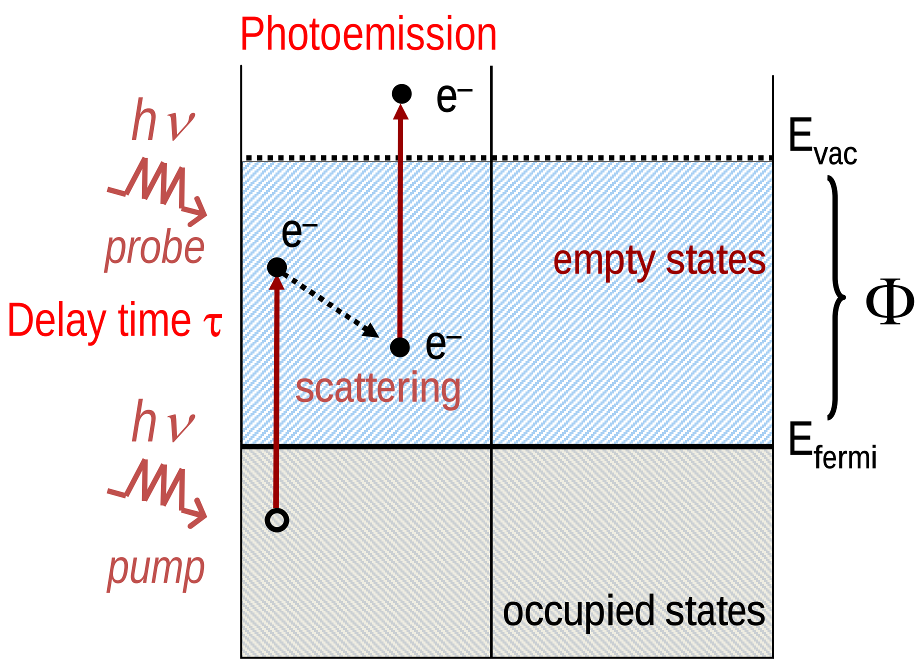

Decay dynamics of non-equilibrium electron distribution in Au film:

PUMP: $h\nu$=1.84eV, I_{abs}=120 $\mu J/cm^2$

PROBE: $h\nu$=5.52eV

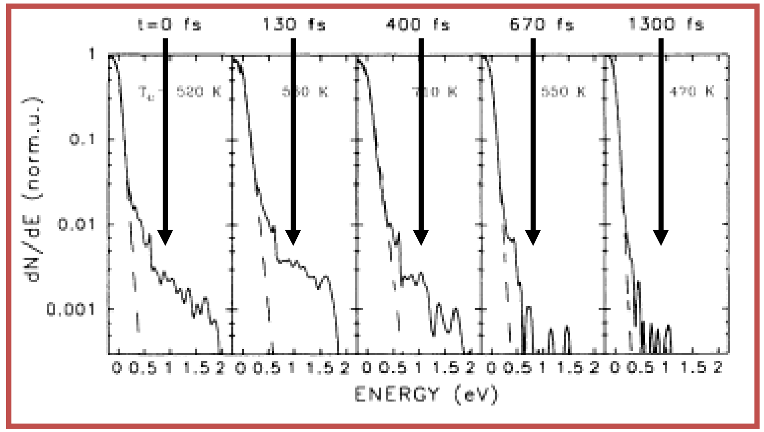

W.S. Fann et al., *Phys. Rev B* 46, 13592 (1992).

Detecting the unoccupied states

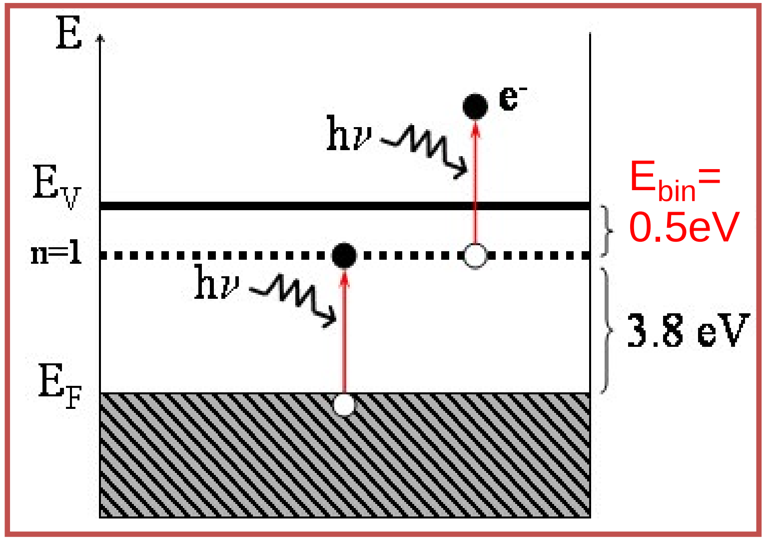

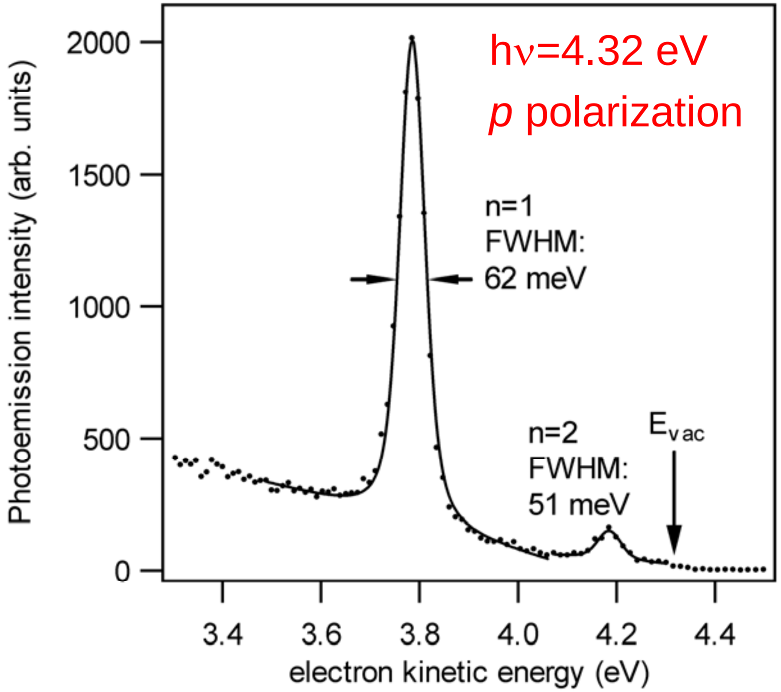

Decay times (τ) are obtained from intrinsic linewidths (Γ) : $\tau = h/\Gamma$

Lifetime at $k_{//}$=0

n =1 Γ=14 ± 2 meV

τ = 47± 7 fs

n=2 Γ= 6 ± 6 meV

τ > 55 fs

G. Ferrini et al., Phys. Rev. B **67**, 235407 (2003)

The Image Potential States (IPS)

In most metals exists a gap in the bulk bands projection on the surface. When an electron is taken outside the solid it could be trapped between the Coulomb-like potential induced by the image charge into the solid, and the high reflectivity barrier due the band gap at the surface.

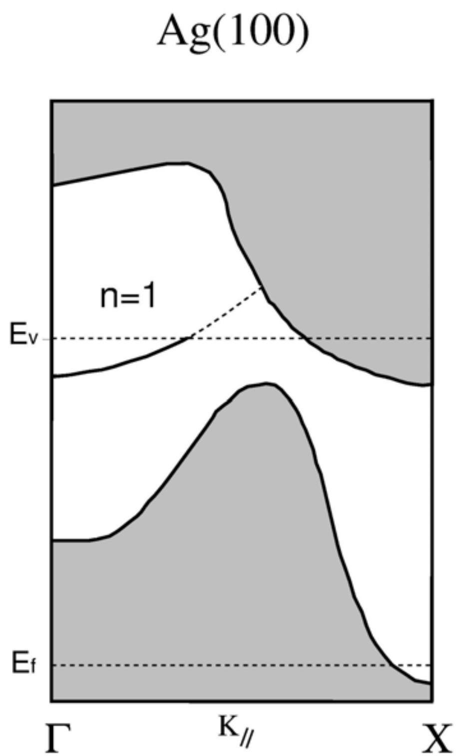

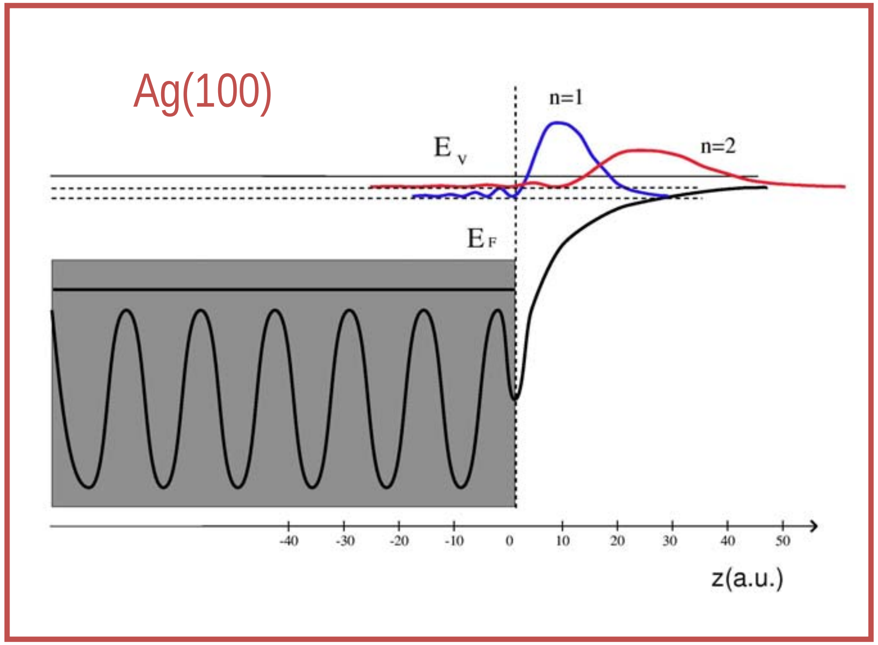

U. Hofer et al., *Science* 277, 1480 (1997).

Selection Rules

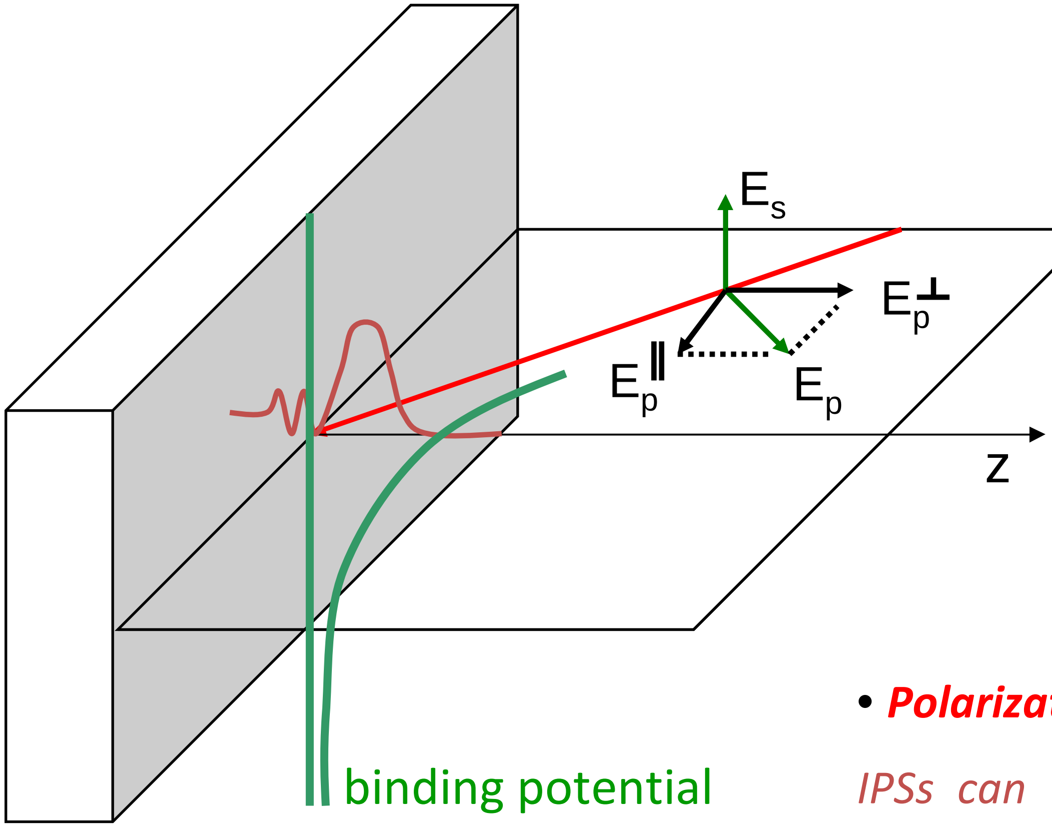

- ***Polarization selection rules***

IPSs can be excited only by the component of the electric field normal to the surface.
Hence, no optical transitions are allowed by s-polarized light

IPS $k_{//}$ Dispersion

LEED

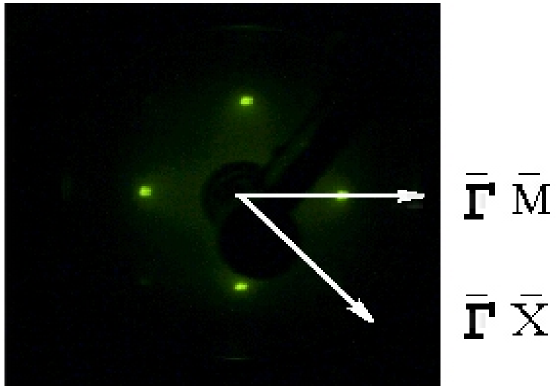

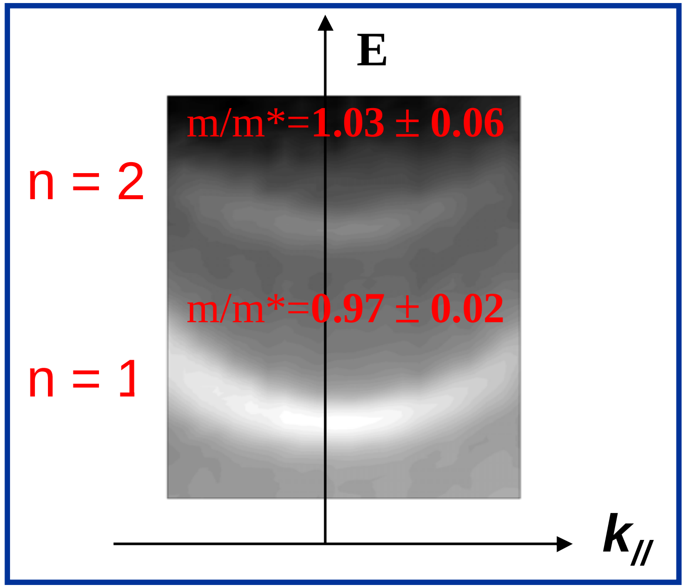

Image Potential States dispersion measured via two-photon resonant ARPES on Ag(100) along $\overline{\Gamma X}$

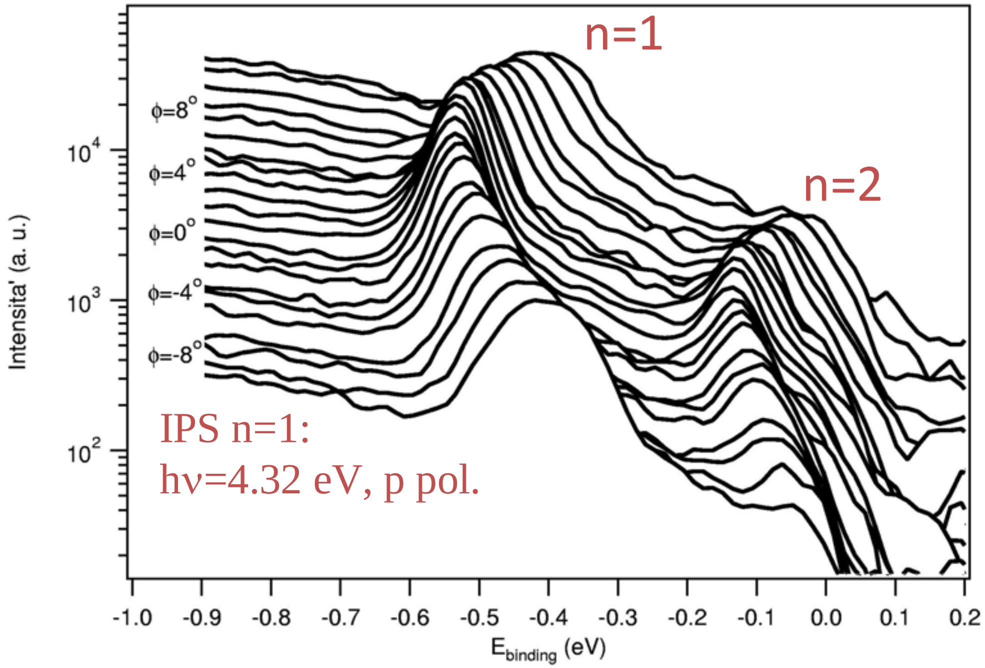

G. Ferrini et al., Phys. Rev. B **67**, 235407 (2003)

$$E_{kin} = h\nu - E_B - \Phi$$

$$k_{//} = \sqrt{2mE_{kin}/\hbar^2} \cdot \sin\theta$$

$$E(n, k_{\parallel}) = \frac{0.85}{(n+a)^2} + \frac{\hbar^2 k_{\parallel}^2}{2m^*}$$

Test of the SR-TR ToF on the Au(111) surface states

- ✓TR- and AR-Photoemission
- ✓Time and Spin resolved experiments
- ✓Fermi surface mapping

Spin-orbit coupling $H_{SO} = \frac{1}{2c^2}\vec{S}\cdot(\vec{\nabla}V\times\vec{p})$

$$V(\vec{r}) = V_0(r,z) + V_3(r,z)\sin 3\varphi + V_6(r,z)\cos 6\varphi$$

$$\vec{\nabla}V = \alpha\,\vec{z} + \beta\,\vec{u}_\varphi \qquad \vec{p} = p\,\vec{u}_r$$

$$H_{SO} = \frac{p}{2c^2}(\alpha\vec{S}\cdot\vec{u}_\varphi + \beta\cos 3\varphi\,\vec{S}\cdot\vec{u}_z)$$

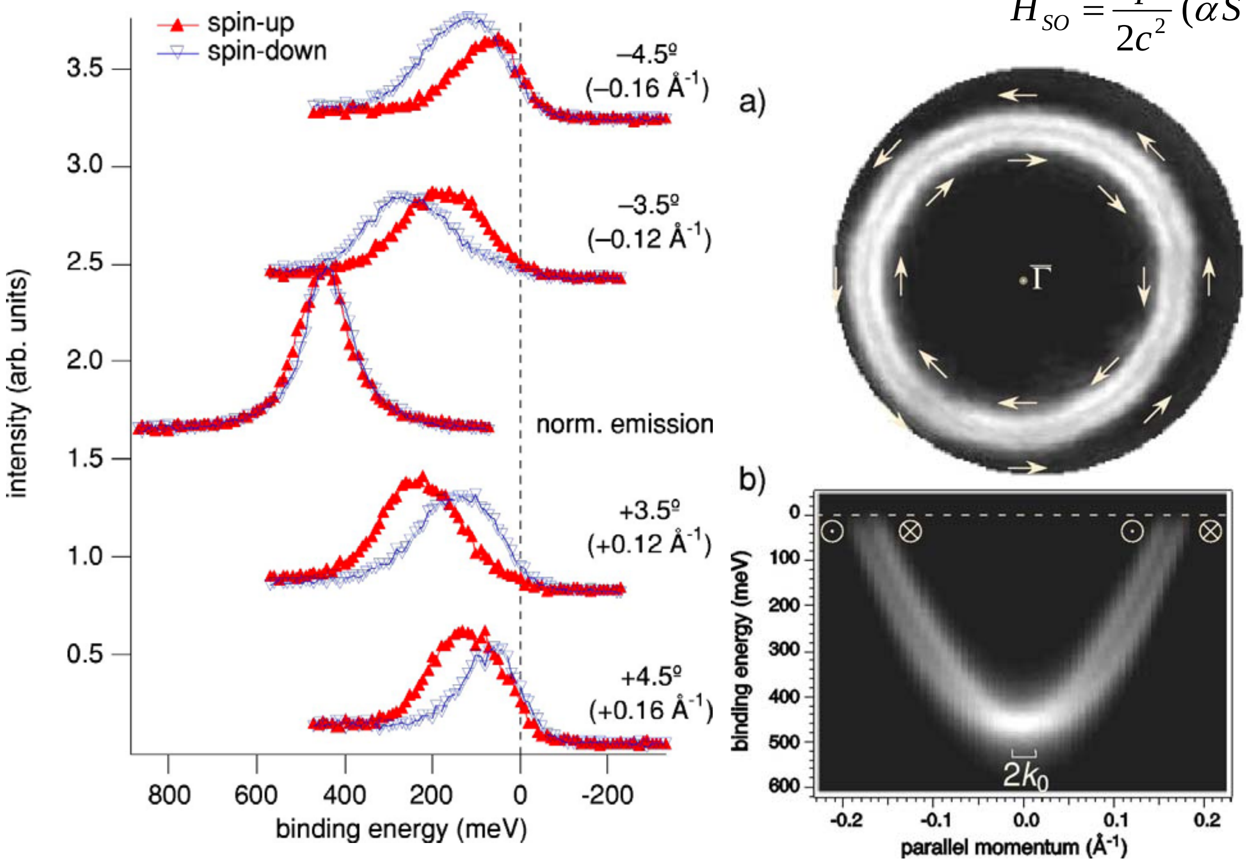

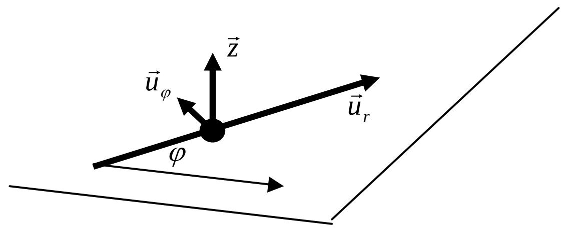

Osterwalder et al. PRB 69 pp.241401R, 2004)

Test of the SR-TR ToF on the Au(111) surface states

Total time = 2h (2 min/scan)
Teta = +/- 22 deg
Low angle resolution

E_0 = 0.26 eV
m^* = 0.134
k_0 = 0.011 Å^{-1}

Vacuum level = 5.49 eV

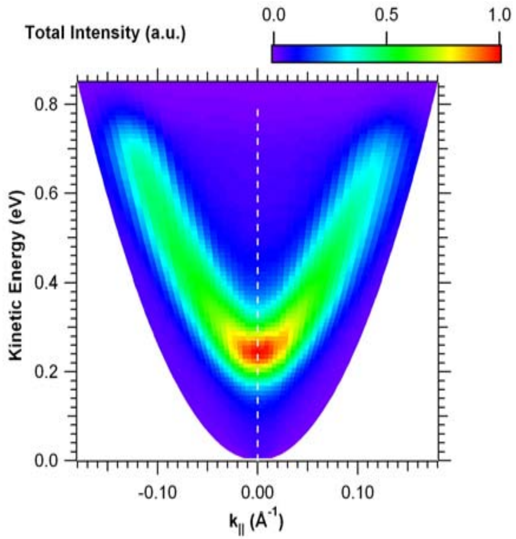

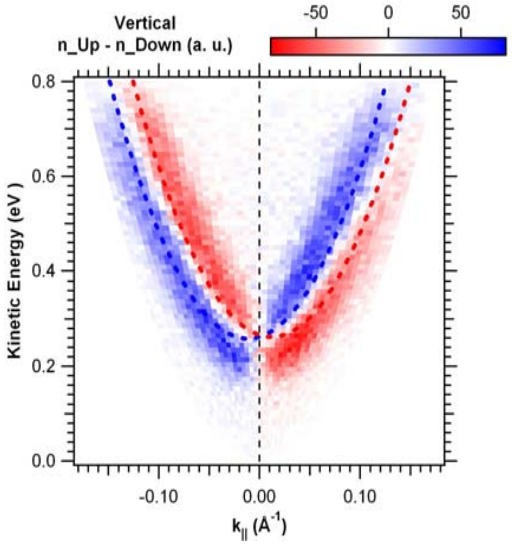

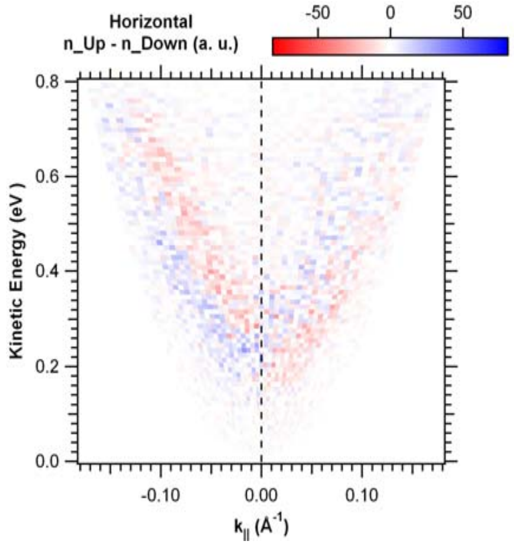

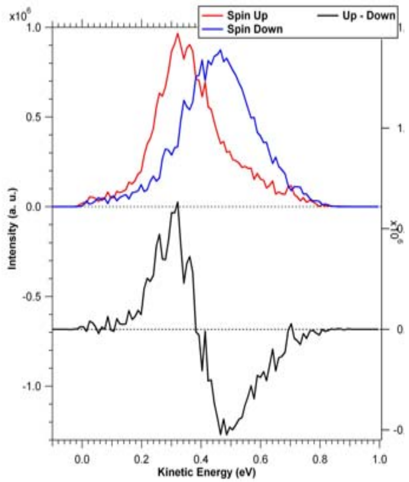

Comparison between the 1kHz and 250kHz laser system

1kHz laser system
Total time = 4h
Total statistic = 4*23400 e-

250 kHz laser system
Total time = **1’ 20’’**
Total statistic = 4*22400 e-

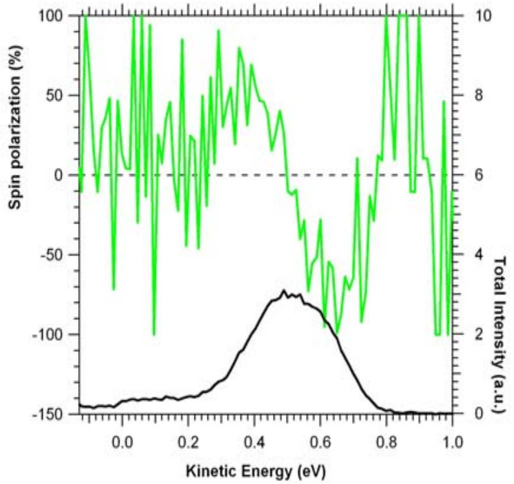

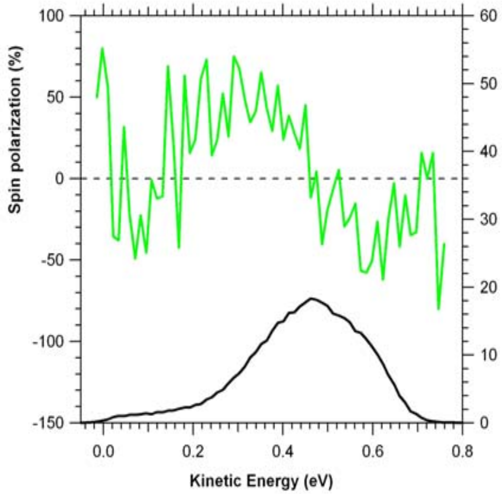

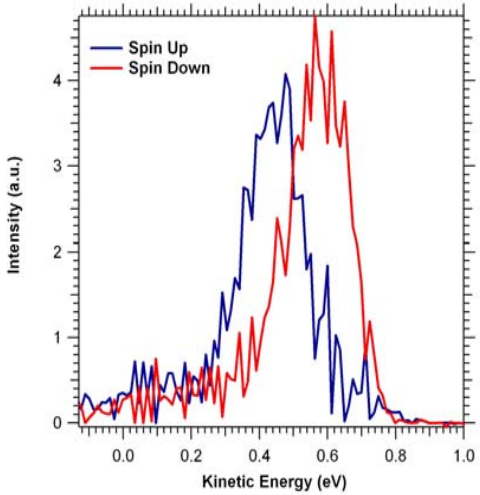

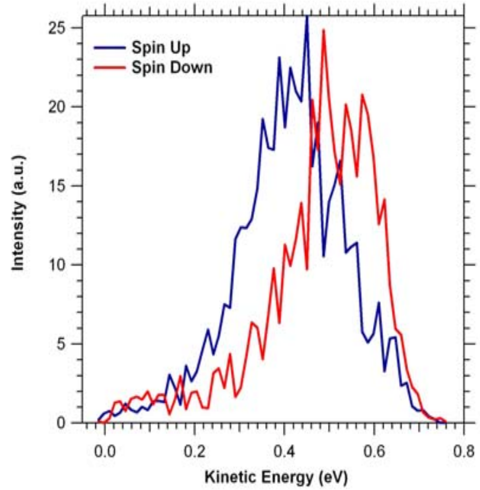

Space Charge Effects

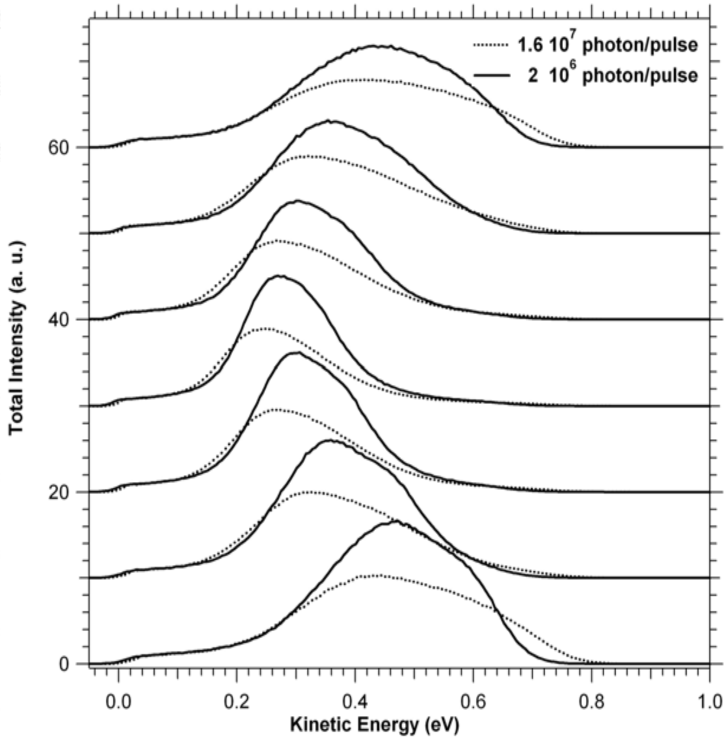

The space charge problem

PHYSICAL REVIEW B 79, 035402 (2009)

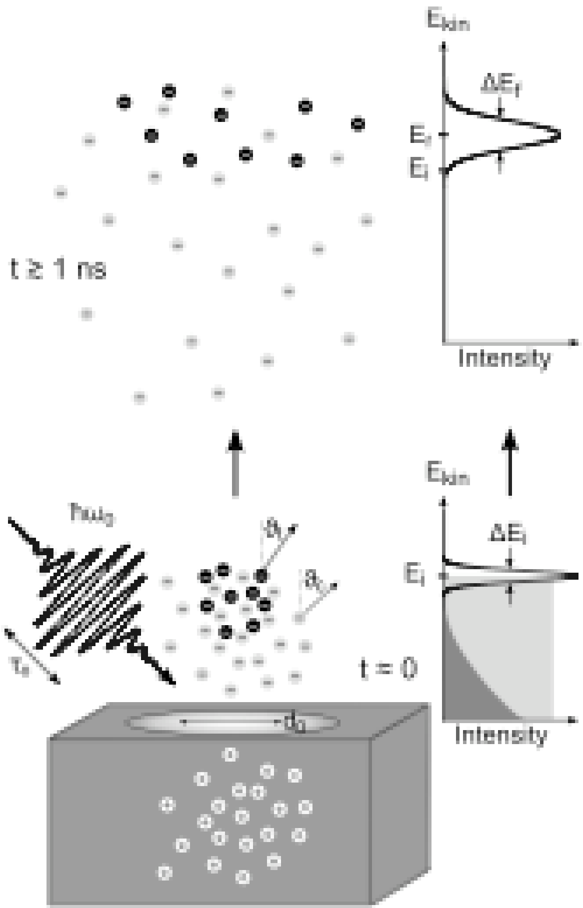

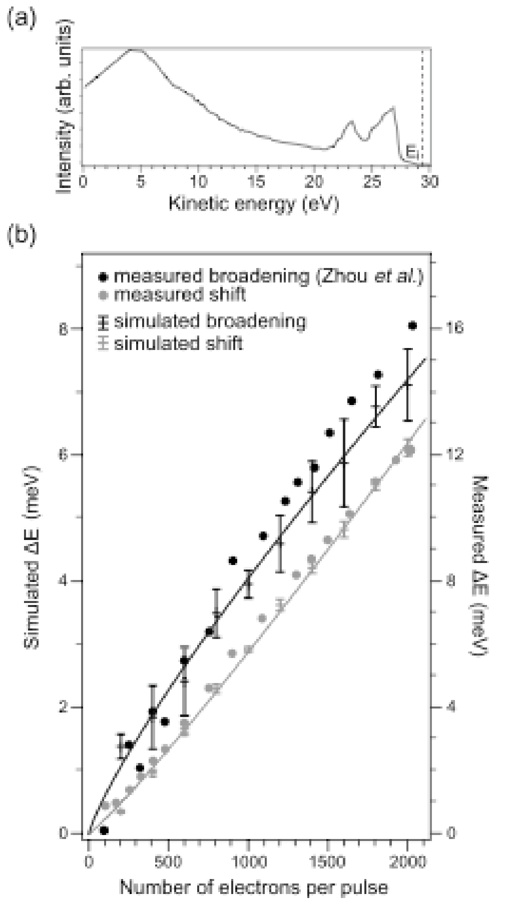

FIG. 3. Space-charge effects on the photoemission spectrum of a polycrystalline gold sample under irradiation with $\tau_0 = 60$ ps, $\hbar\omega_0 = 34$ eV photon pulses. (a) Typical energy distribution curve with the Fermi cutoff at 29.38 eV (taken from Ref. 9). (b) Comparison between simulated and measured (Ref. 9) Fermi edge shifts and broadenings in the range of $(0-2000)e^-$ per pulse. Note the different scales of the vertical axes. Power-law fits to the simulated energy shift and broadening serve as guides for the eyes ($\Delta E_{shift} \propto N_c^{1.11}, \Delta E_{broad} \propto N_c^{0.83}$). The spot size is 0.43×0.3 mm^2 and the test electrons are emitted with an angle of 45°. In the simulation, a cosine distribution of the cloud electron emission angles is used.

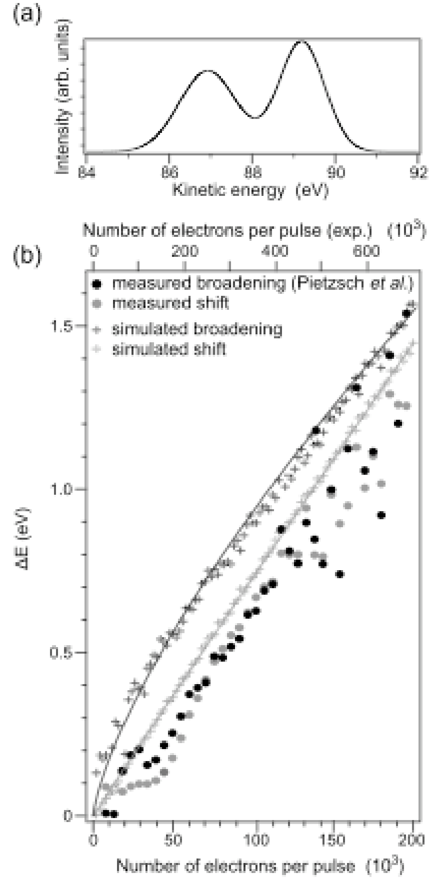

FIG. 5. Space-charge effects on a W 4f core-level spectrum under irradiation with $\tau_0 = 40$ fs, $\hbar\omega_0 = 118.5$ eV photon pulses. (a) Typical energy distribution curve with photoemission peaks at kinetic energies of ~87 and ~89 eV (taken from Ref. 21). (b) Comparison between simulated and measured (Ref. 21) peak shifts and broadenings in the range of $(0-200\,000)e^-$ per pulse. Note the different scales of the axes for the simulated (bottom axis) and measured data (top axis). Power-law fits to the simulated energy shift and broadening serve as guides for the eyes ($\Delta E_{shift} \propto N_c^{0.98}, \Delta E_{broad} \propto N_c^{0.75}$). The spot size is 0.27×0.4 mm^2. In the simulation, a cosine distribution of the cloud electron emission angles is used and the test electron acceptance angle is set to 13°.

The escape depth question

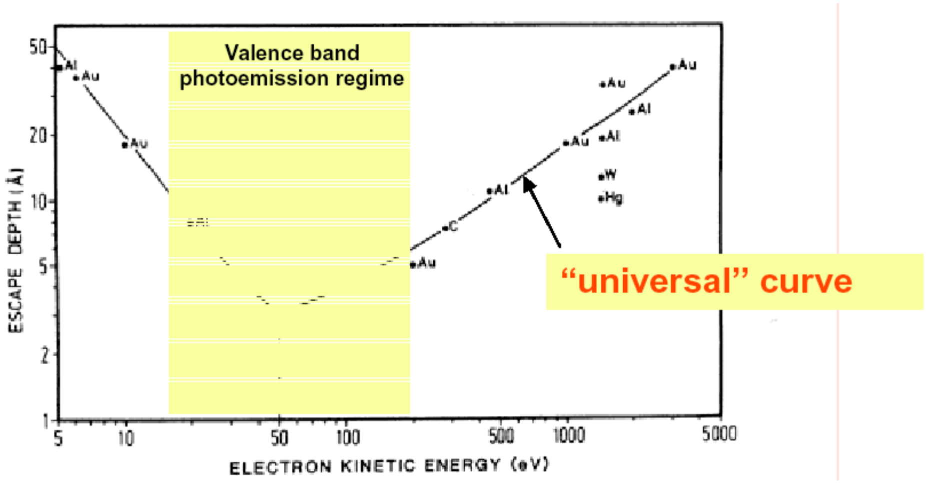

C1s, O1s and

Pt4f XPS

CO adsorption

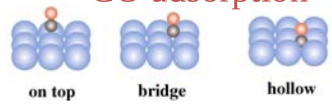

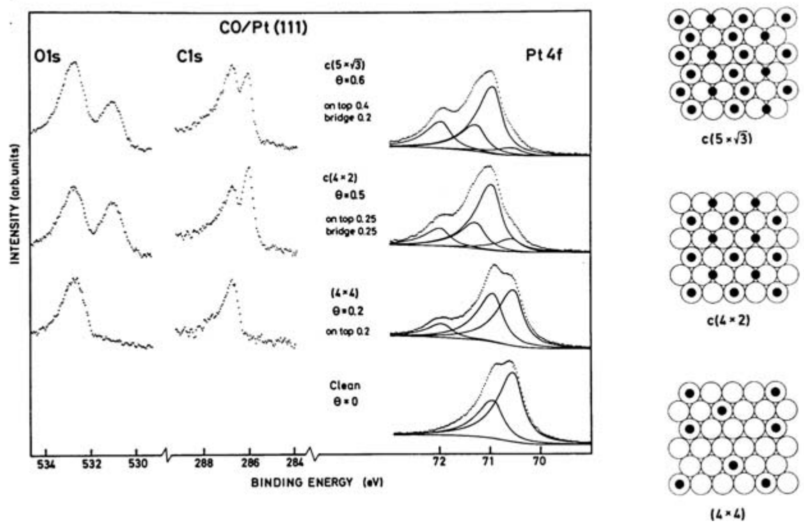

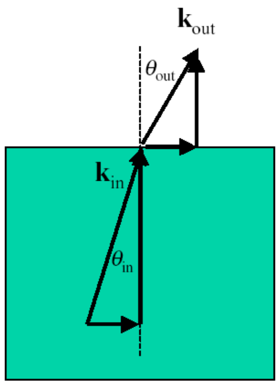

Kinematic relations

$$k_{out} = \sqrt{\frac{2m}{\hbar^2} E_{kin}}$$

$$k_{in} = \sqrt{\frac{2m}{\hbar^2} (E_{kin} + V_0)}$$

$$k_{out,\parallel} = k_{in,\parallel} \equiv k_{\parallel}$$

"Snell's Law"

$$k_{\parallel} = \sin\theta_{out} \sqrt{\frac{2m}{\hbar^2} E_{kin}} = \sin\theta_{in} \sqrt{\frac{2m}{\hbar^2} (E_{kin} + V_0)}$$

Critical angle for emission

$$(\sin\theta_{out})_{\max} = \sqrt{\frac{E_{kin}}{E_{kin} + V_0}}$$

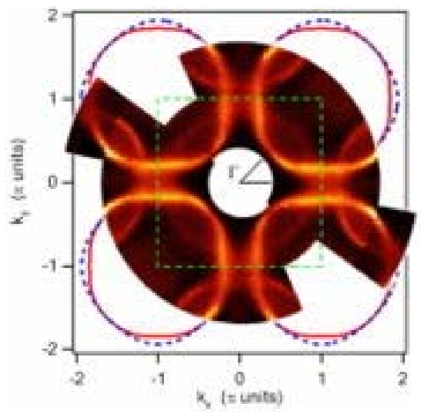

Fermi surface of BSCCO measured by ARPES. The experimental data shown as an intensity plot in yellow-red-black scale. Green dashed rectagle represents the Brillouin zone of the CuO2 plane of BSCCO.

The escape depth question

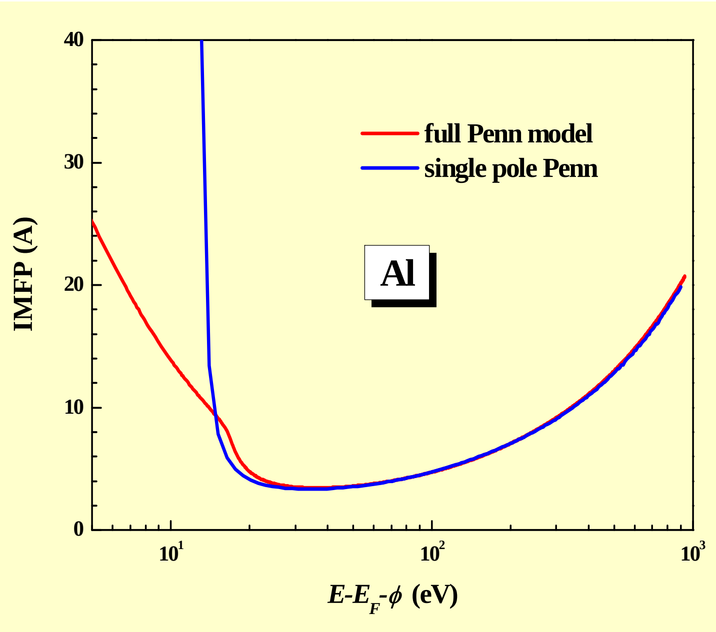

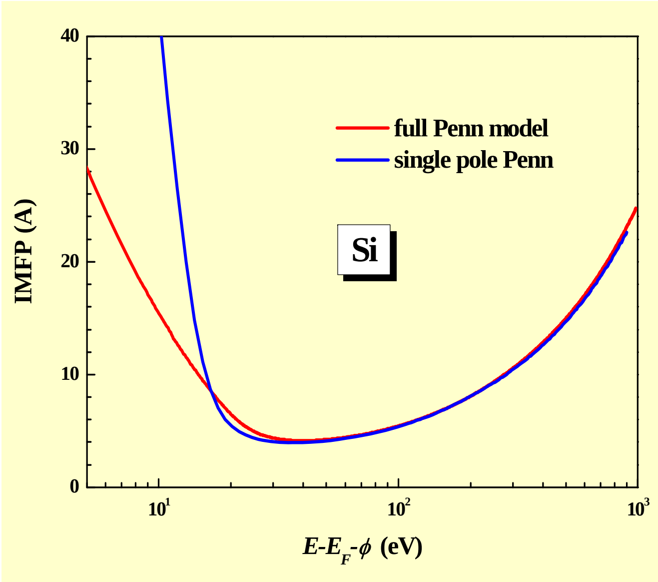

More realistic look at low-energy inelastic mean free paths--theory

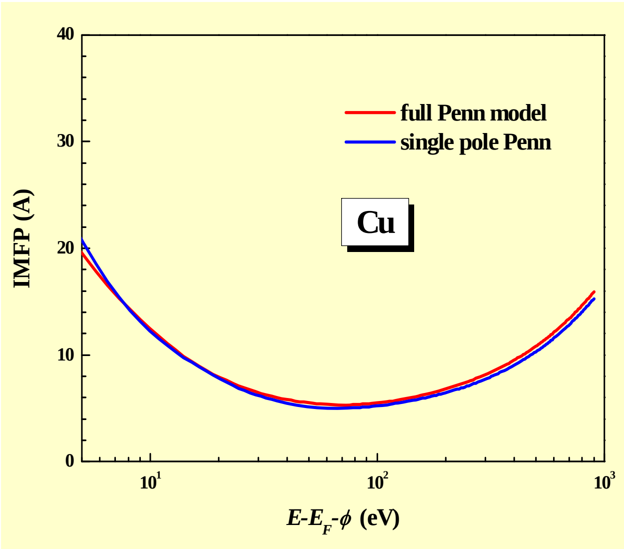

S.F. Mao and Z.J. Ding, Hefei (TBP)

VOLPE project:
VOLume PhotoEmission with Synchotron Radiation

Team:

INFM-Lab. TASC
ELETTRA
Univ. Rome III,
EPFL
LURE
ESRF (ID16)

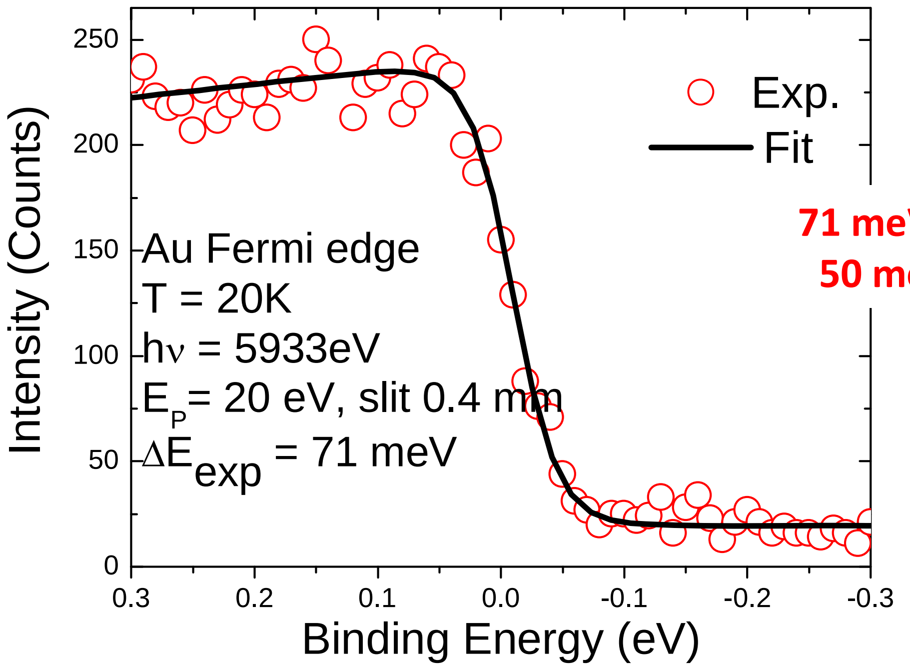

71 meV @ 5933 eV
50 meV analyser

Panaccione et al. NIMA (2005)
Torelli et al., Rev.Sci. Instr. 76, 023909 (2005)

High Resolution /High Flux beamline: ID16 @ ESRF

An outlook to the present and to the future

PRL 96, 017005 (2006) PHYSICAL REVIEW LETTERS week ending 13 JANUARY 2006

Laser Based Angle-Resolved Photoemission, the Sudden Approximation, and Quasiparticle-Like Spectral Peaks in $Bi_2Sr_2CaCu_2O_{8+\delta}$

J. D. Koralek,[1,2,*] J. F. Douglas,[1] N. C. Plumb,[1] Z. Sun,[1,3] A. V. Fedorov,[3] M. M. Murnane,[1,2] H. C. Kapteyn,[1,2] S. T. Cundiff,[2] Y. Aiura,[4] K. Oka,[4] H. Eisaki,[4] and D. S. Dessau[1,2,†]

PRL 97, 067402 (2006) PHYSICAL REVIEW LETTERS week ending 11 AUGUST 2006

Time Evolution of the Electronic Structure of 1*T*-TaS_2 through the Insulator-Metal Transition

L. Perfetti,[1] P. A. Loukakos,[1] M. Lisowski,[1] U. Bovensiepen,[1] H. Berger,[2] S. Biermann,[3] P. S. Cornaglia,[3] A. Georges,[3] and M. Wolf[1]

PRL 99, 197001 (2007) PHYSICAL REVIEW LETTERS week ending 9 NOVEMBER 2007

Ultrafast Electron Relaxation in Superconducting $Bi_2Sr_2CaCu_2O_{8+\delta}$ by Time-Resolved Photoelectron Spectroscopy

L. Perfetti,[1] P. A. Loukakos,[1] M. Lisowski,[1] U. Bovensiepen,[1] H. Eisaki,[2] and M. Wolf[1]
[1]*Fachbereich Physik, Freie Universität Berlin, Arnimallee 14, 14195 Berlin, Germany*
[2]*AIST Tsukuba Central 2, 1-1-1 Umenzono, Tsukuba, Ibaraki 305-8568, Japan*
(Received 18 April 2007; published 9 November 2007)

PRL 100, 107002 (2008) PHYSICAL REVIEW LETTERS week ending 14 MARCH 2008

Identification of a New Form of Electron Coupling in the $Bi_2Sr_2CaCu_2O_8$ Superconductor by Laser-Based Angle-Resolved Photoemission Spectroscopy

Wentao Zhang,[1] Guodong Liu,[1] Lin Zhao,[1] Haiyun Liu,[1] Jianqiao Meng,[1] Xiaoli Dong,[1] Wei Lu,[1] J. S. Wen,[2] Z. J. Xu,[2] G. D. Gu,[2] T. Sasagawa,[3] Guiling Wang,[4] Yong Zhu,[5] Hongbo Zhang,[4] Yong Zhou,[4] Xiaoyang Wang,[5] Zhongxian Zhao,[1] Chuangtian Chen,[5] Zuyan Xu,[4] and X. J. Zhou[1,*]

An outlook to the present and to the future

Selective excitations (CT and phonons) to study transient states and photo-induced phase transitions.
Superconductors (e-ph interactions, magnetism and superconductivity).
Magnetic materials (dynamics of the magnetic excitations).
Strong correlations in hard- and soft- condensed matter (charge transfer and phonon assisted excitations).

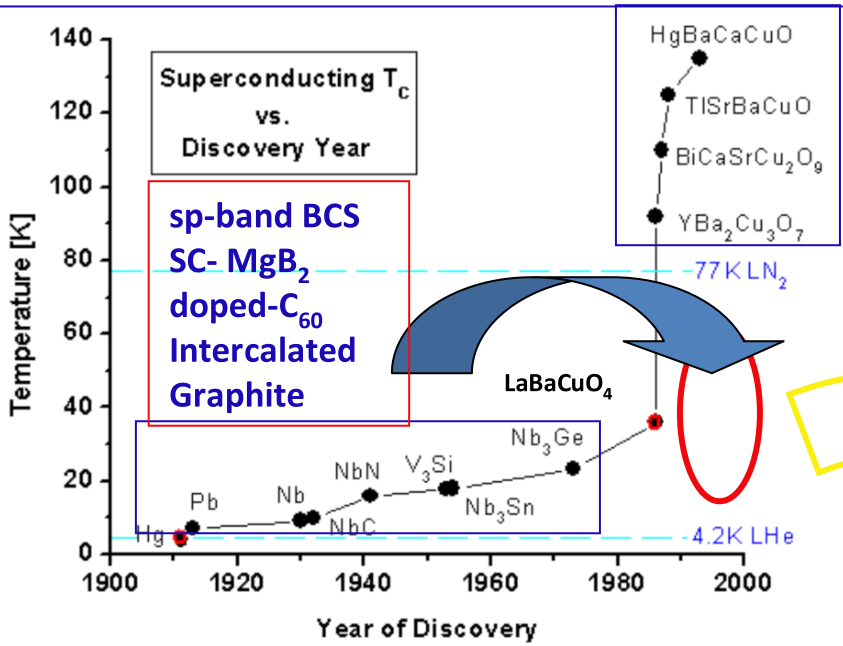

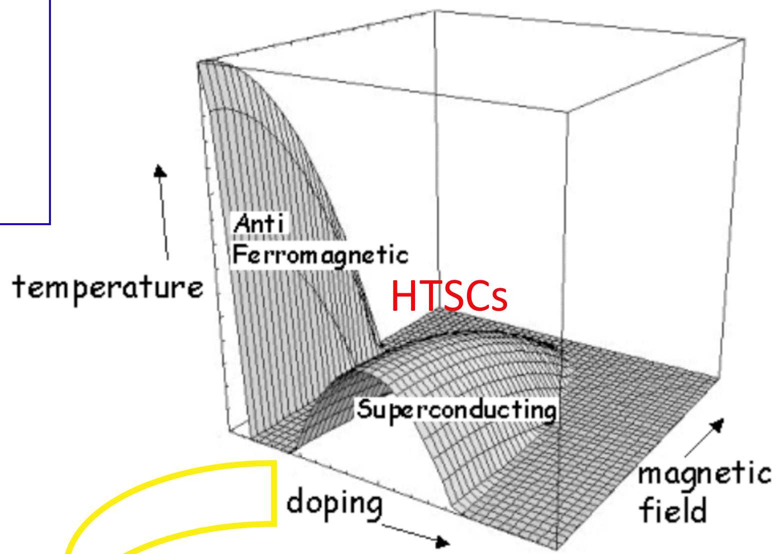

e-ph

?

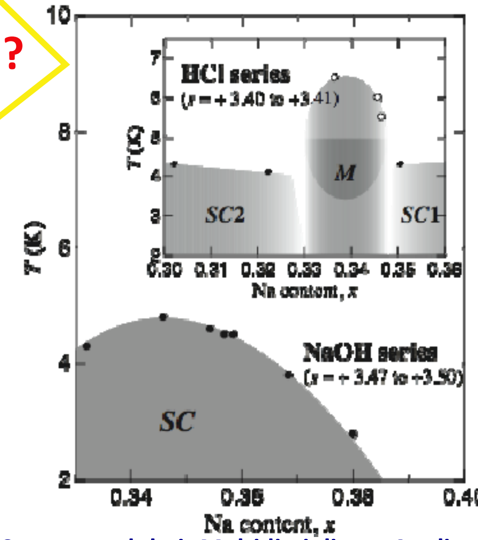

$$\lambda_{\nu \mathbf{q}} \equiv \frac{1}{\pi N(0)} \frac{\gamma_{\nu \mathbf{q}}}{\omega^2_{\nu \mathbf{q}}}. \qquad N_n(0) \equiv \sum_{\mathbf{k}} \delta(\varepsilon_{n\mathbf{k}})$$

$$\frac{\gamma_{\nu \mathbf{q}}}{\omega_{\nu \mathbf{q}}} = 2\pi \sum_{nm\mathbf{k}} |g_{\nu,n\mathbf{k},m(\mathbf{k}+\mathbf{q})}|^2 \delta(\varepsilon_{n\mathbf{k}})\delta(\varepsilon_{m\mathbf{k}+\mathbf{q}}).$$

$$g_{\nu,n\mathbf{k},m(\mathbf{k}+\mathbf{q})} = \langle n\mathbf{k}|\delta V(\mathbf{r})|m(\mathbf{k}+\mathbf{q})\rangle / \delta Q_{\nu \mathbf{q}}$$

Photoemission on low density matter

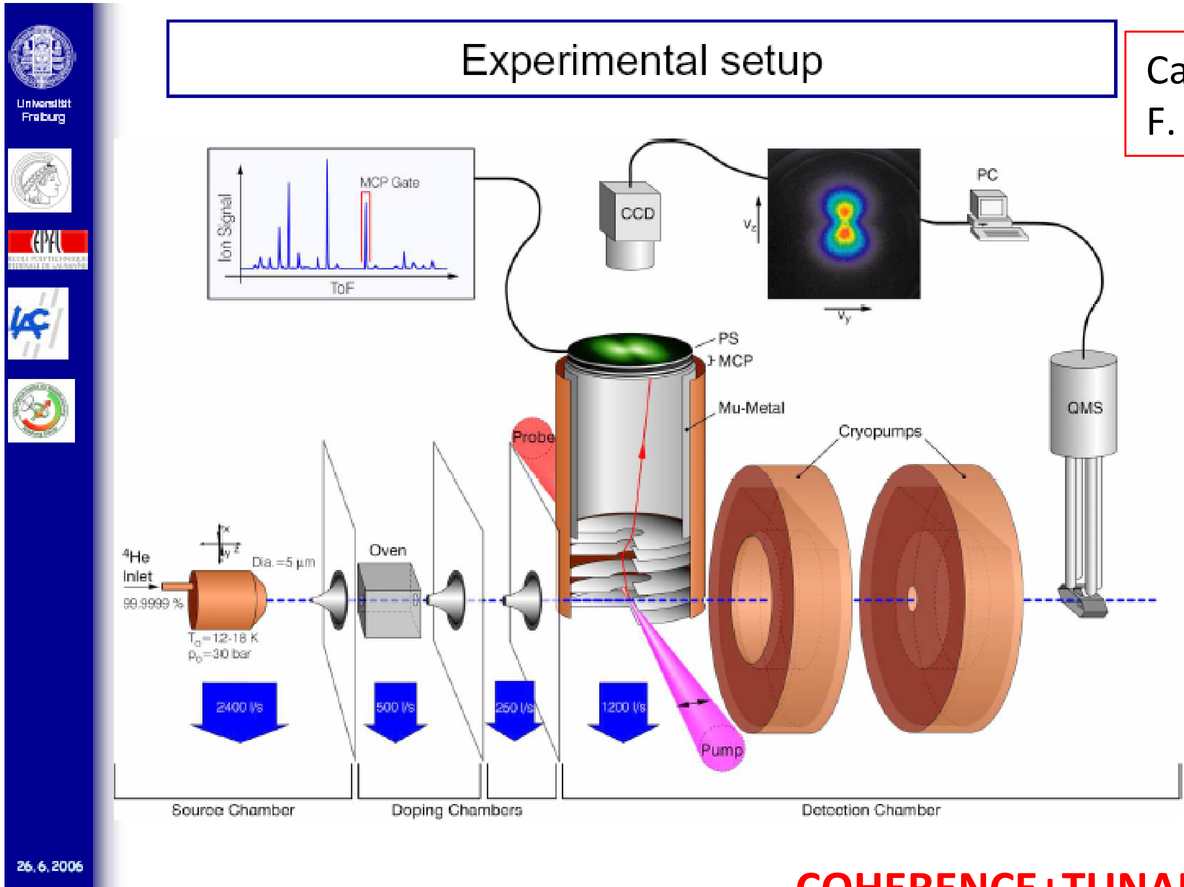

Carlo Callegari: LDM coordinator
F. Stienkemeir: End station spoke person

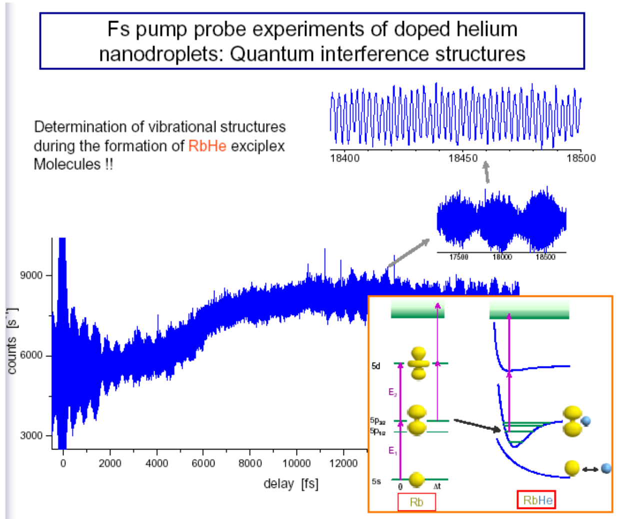

COHERENCE+TUNABILITY+POLARIZATION

Cluster and nanoparticle spectroscopy

Spokespersons: **F. Stienkemeier,** (Univ. of Freiburg-D); **T. Moeller** (Frei University, Berlin)
Co-proponents :K.Fauth (MPI- Stuttgart, D), M. Drabbels (EPFL- CH), M. Schmidt(CNRS –Orsay, Fr), U.Buck (MPI-Goettingen, D)

An outlook to the present and to the future

Dynamics of the volume collapse

alpha-gamma phase transition in cerium:
- Promotional Model ?
- Mott transition ?
- Kondo Volume Collapse ?

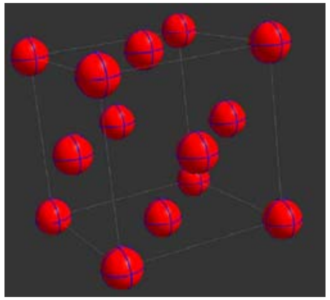

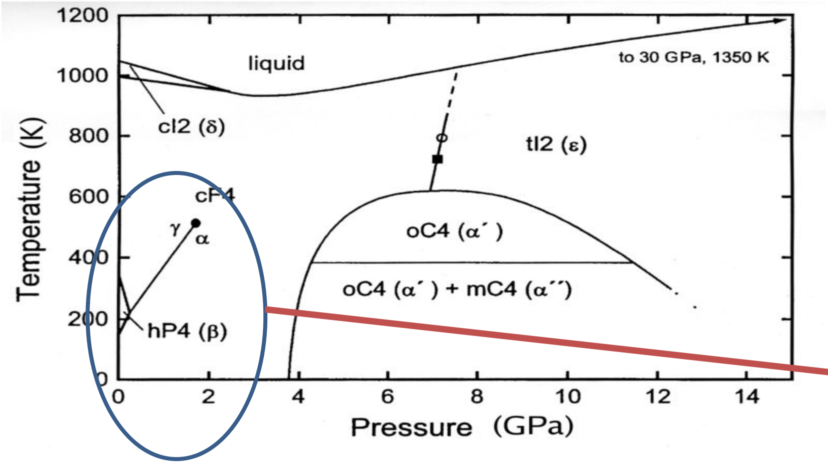

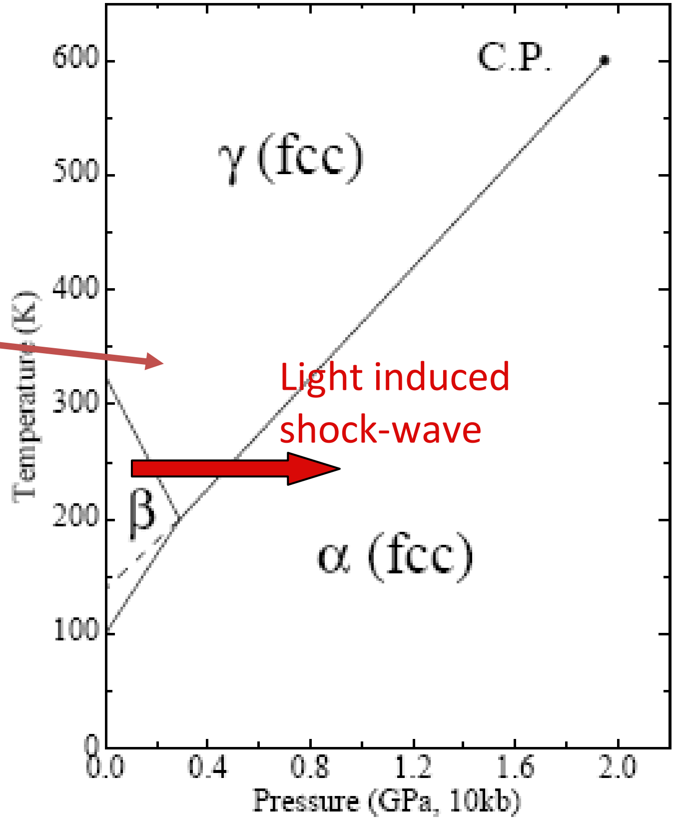

fcc-fcc isostructural transition:

1.15% volume collapse

cell-length : 5.1612 → 4.677

cell-volume : 137.4 → 102.3

symmetry: F m -3 m

2.Curie Weiss magnetism-Pauli Magnetism (zero moment)

The 10^{-18} s Challenge with 0.1-1 keV soft X-ray

Attosecond science

Nature Physics, June 2007

The motion of electrons on the atomic scale has been hidden from direct experimental access until recently. We review the revolution in technology that opened the door to real-time observation and time-domain control of atomic-scale electron dynamics, and address the expected implications of having the tools to monitor electrons with sub-atomic resolution in both space and time.

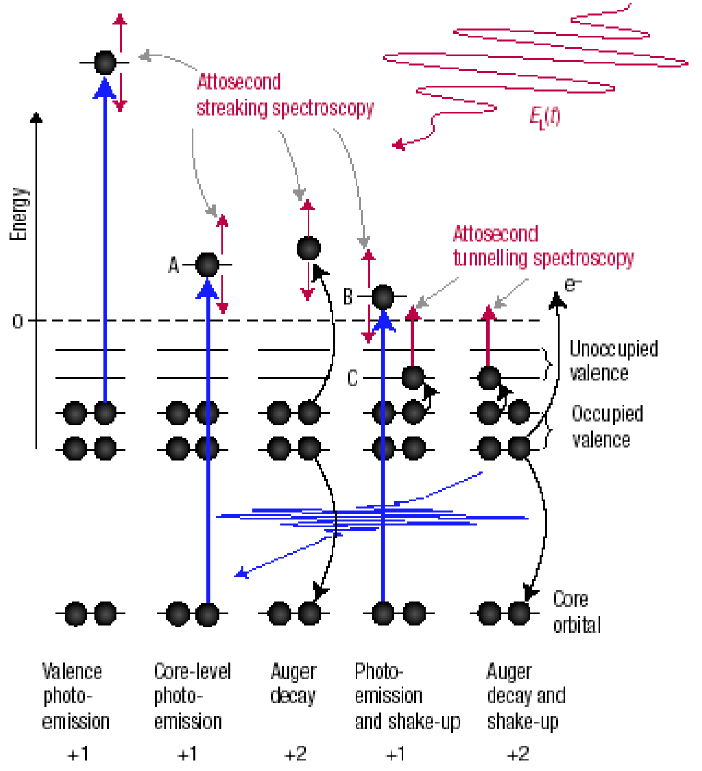

Excitation and relaxation. Electronic excitation and relaxation processes in atoms, molecules and solids, and possible ways of tracing these dynamics in real time. The labels 1+ and 2+ indicate single and double ionization.

10 AUGUST 2007 VOL 317 SCIENCE

Attosecond Spectroscopy

REVIEW

The Future of Attosecond Spectroscopy

Philip H. Bucksbaum

Attoscience is the study of physical processes that occur in less than a fraction of a cycle of visible light, in times less than a quadrillionth of a second. The motion of electrons inside atoms and molecules that are undergoing photoionization or chemical change falls within this time scale, as does the plasma motion that causes the reflectivity of metals. The techniques to study motion on this scale are based on careful control of strong-field laser-atom interactions. These techniques and new research opportunities in attosecond spectroscopy are reviewed.

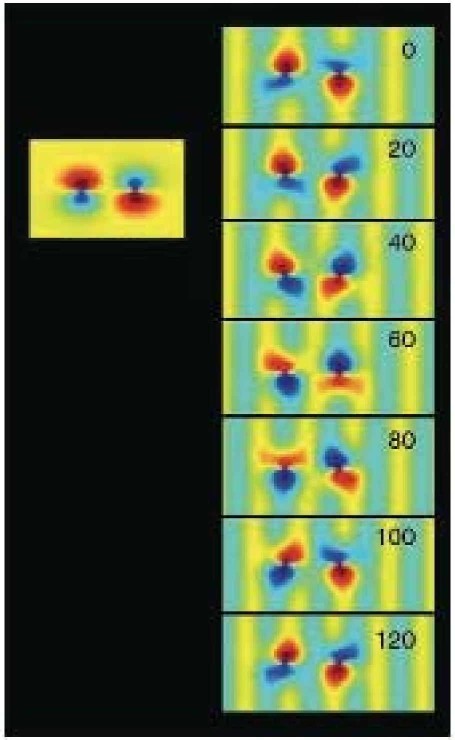

Fig. 2. (Left) Wave function simulating the most weakly bound electron in carbon dioxide, consisting of two p_x orbitals separated by 2.32 Å. Red and blue parts of the wave function are π radians apart in quantum phase. (Right) Coherent scattering of a 25-eV electron from the carbon dioxide orbital out of which it was recently ejected by a strong laser field. The returning electron is incident from the right, and several views are shown over a 120-as time interval. The relative time (in attoseconds) is shown in the top right of the frames. Motion of the wave function is due to interference with the incoming electron.

NL-ARPES EXPERIMENTAL SETUP

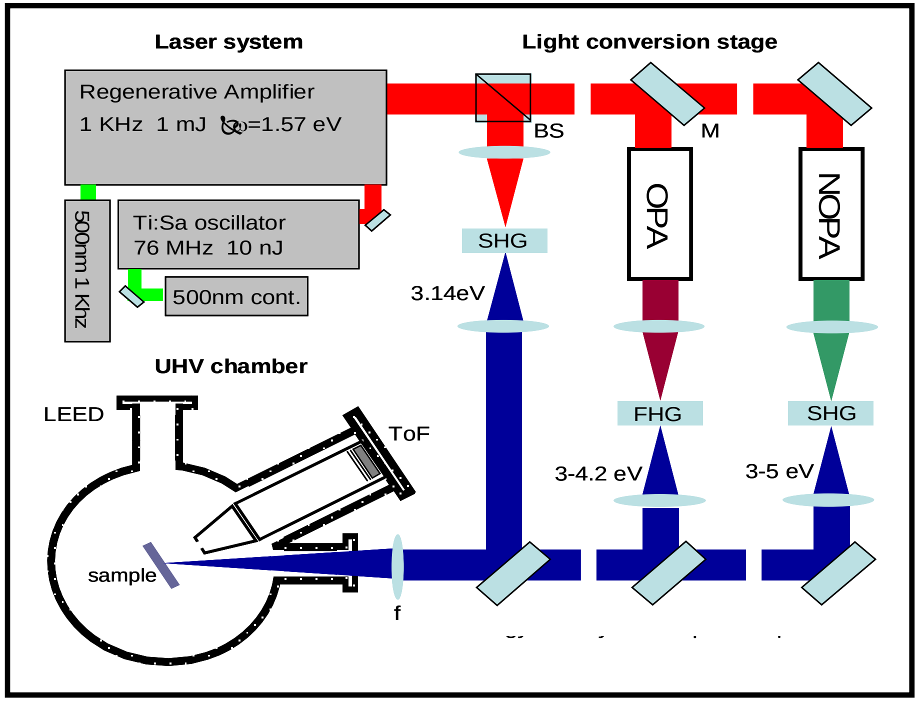

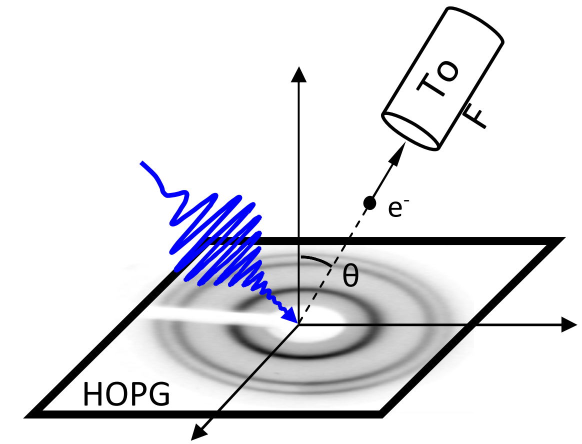

ToF PARAM : Acc. Angle : ± 0.83°

ΔE = 30meV @ 2 eV E_K

P < 2 10^{-10} mbar, T=300 K

120 fs; 1 KHz Rep. Rate $\hbar\omega$=3 – 5 eV ; F~100 μJ cm^{-2}

High intensity (>GW cm^{-2}), Spatially coherent light pulses
Pulse duration (120fs) << π* excitation lifetime (ps)

ACCESS TO THREE IPS QUANTITIES :

IPS PE YIELD - IPS LINEWIDTH - IPS EFFECTIVE MASS

BULK STRUCTURE of GRAPHITE

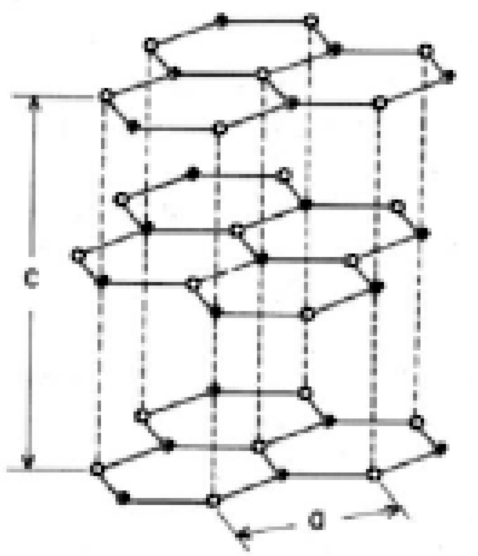

Optically active in the 3-4 eV region, due to the π bands

van Hove singularity in the J-DOS due to the π bands

Saddle point @ M point = HIGH ABSORPTION

Anisotropic: Surface excitations diffuse poorly in the bulk

IPS band not fully studied with NL-ARPES

Lehmann, PRB 60, 17037 (1999)

Layered: Possible High IPS-bulk coupling due to the presence of the Interlayer (IL) band

IPS SENSIBLE TO BULK EXCITATIONS

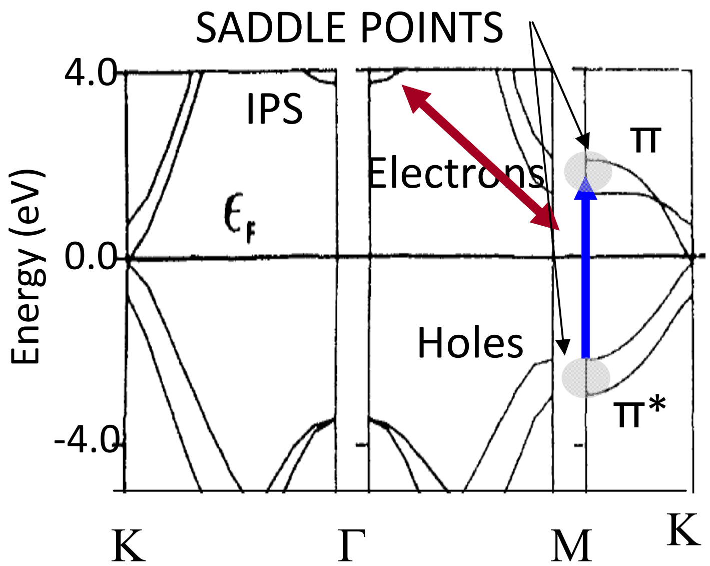

NON-LINEAR PHOTOEMISSION SPECTROSCOPY

INTENSE VIS / NEAR-UV LASER PULSES AS PROBE:
MULTIPHOTON TRANSITIONS (hv < Φ)
ACCESS TO EMPTY & EXCITED STATES

Fauster 2003

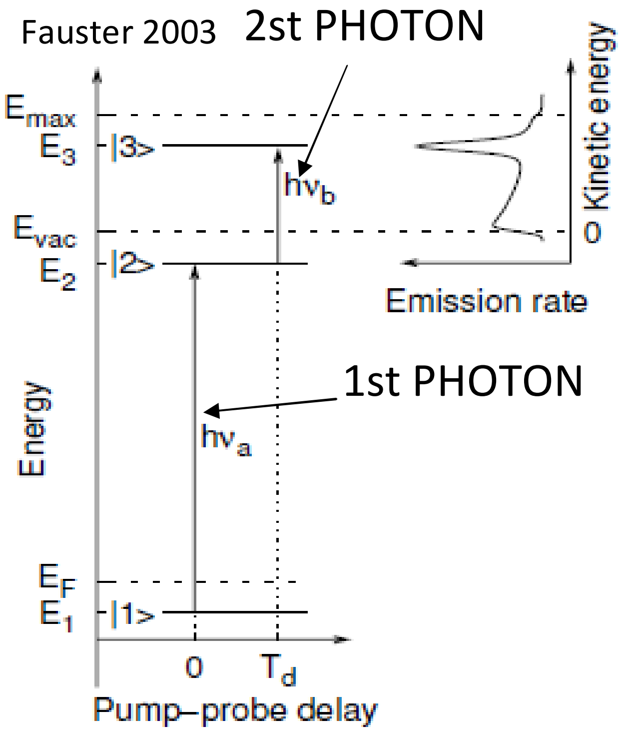

TIME RESOLVED STUDIES

ACCESS to LIFETIMES

OUR REALIZATION: $v_a=v_b$
SINGLE PULSE MODE

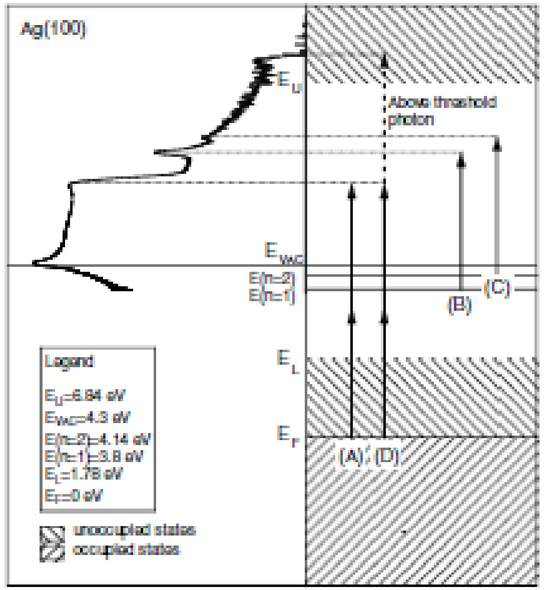

Banfi et al. PRL 94, 037601 (2005)

ABOVE TRESHOLD PHOTOEMISSION IN SOLIDS CONFIRMED USING 3.14 eV PULSES

TWO FEATURES : IPS AND BULK π* SHOULDER

NORMAL EMISSION SPECTRA (A geom)

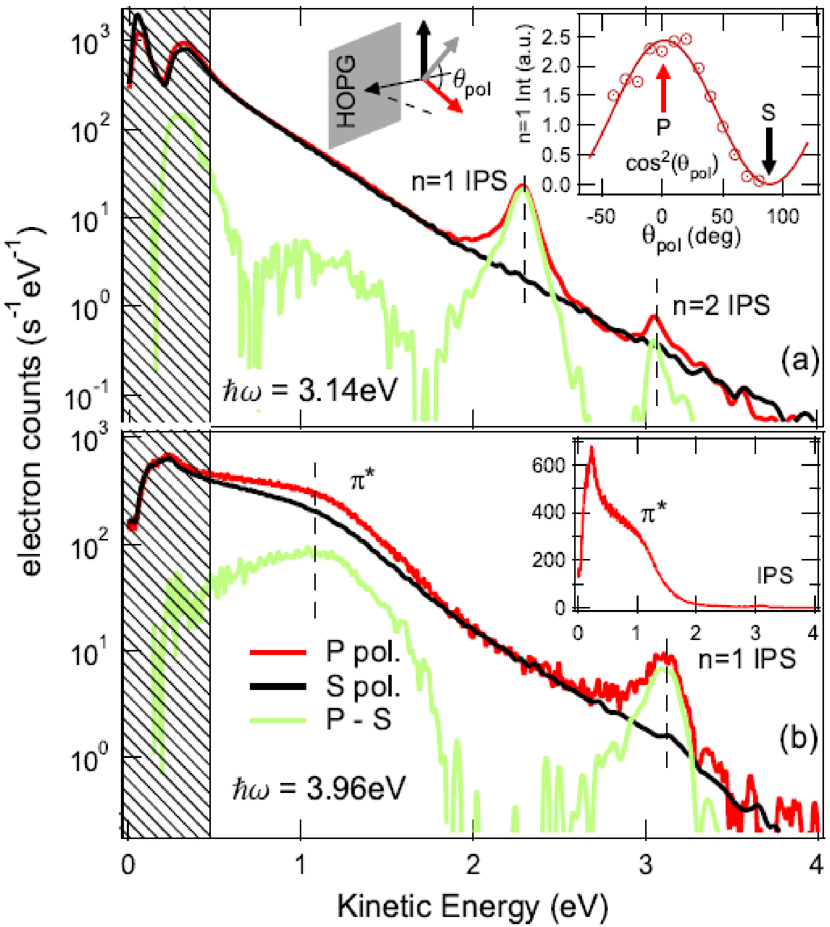

SHIFT WITH PHOTON ENERGY

POLARIZATION SELECTION RULES

IPS photoemitted only by $e_\perp$

$$I(\theta_p) \approx \cos^2(\theta_p)$$

π (σ) photoemitted by $e_\perp$ ($e_{||}$)

IPS QUANTUM DEFECT

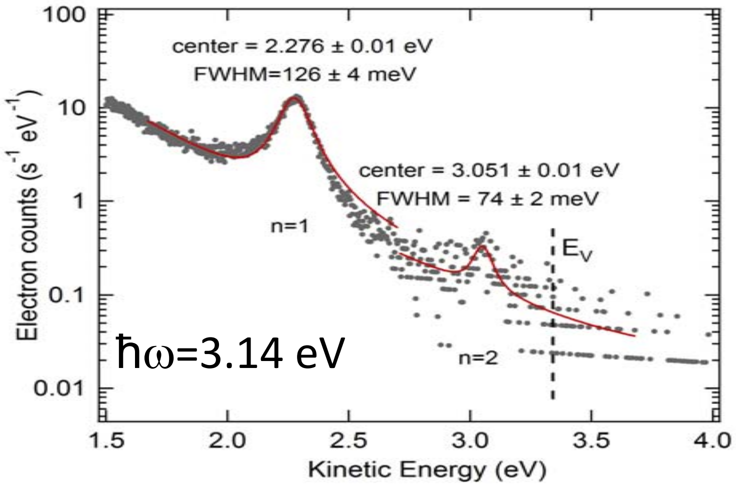

$$\Delta E = \frac{Ry}{16}\left[(1+a)^{-2} - (2+a)^{-2}\right]$$

$$a = -0.08 \pm 0.04$$

MULTIPHOTON TRANSITIONS for IPS AND π*

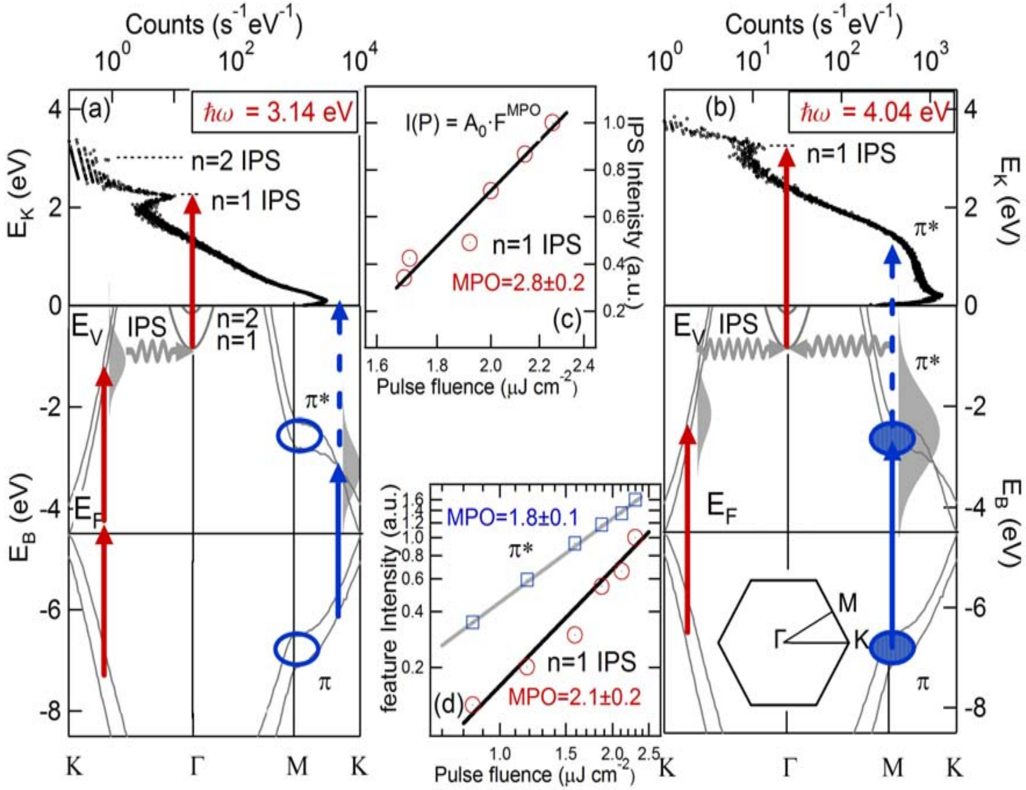

TWO IPS POPULATION PROCESSES

MPO=2+1 = 3

Multi Photon Order

MPO=1+1 = 2

TWO BULK EXCITATION REGIMES

OUT OF RESONANCE

With π, π* SADDLE

IN RESONANCE

IPS IS POPULATED IN A NO-RESONANT WAY BY SCATTERING OF THE HIGH DENSITY OF EXCITED ELECTRONS IN π* BANDS

$n \sim 10^{20}\ cm^{-3}$ @ $F = 100\ \mu J\ cm^{-2}$

VARYING PHOTON ENERGY: STRUCTURE in IPS and π*

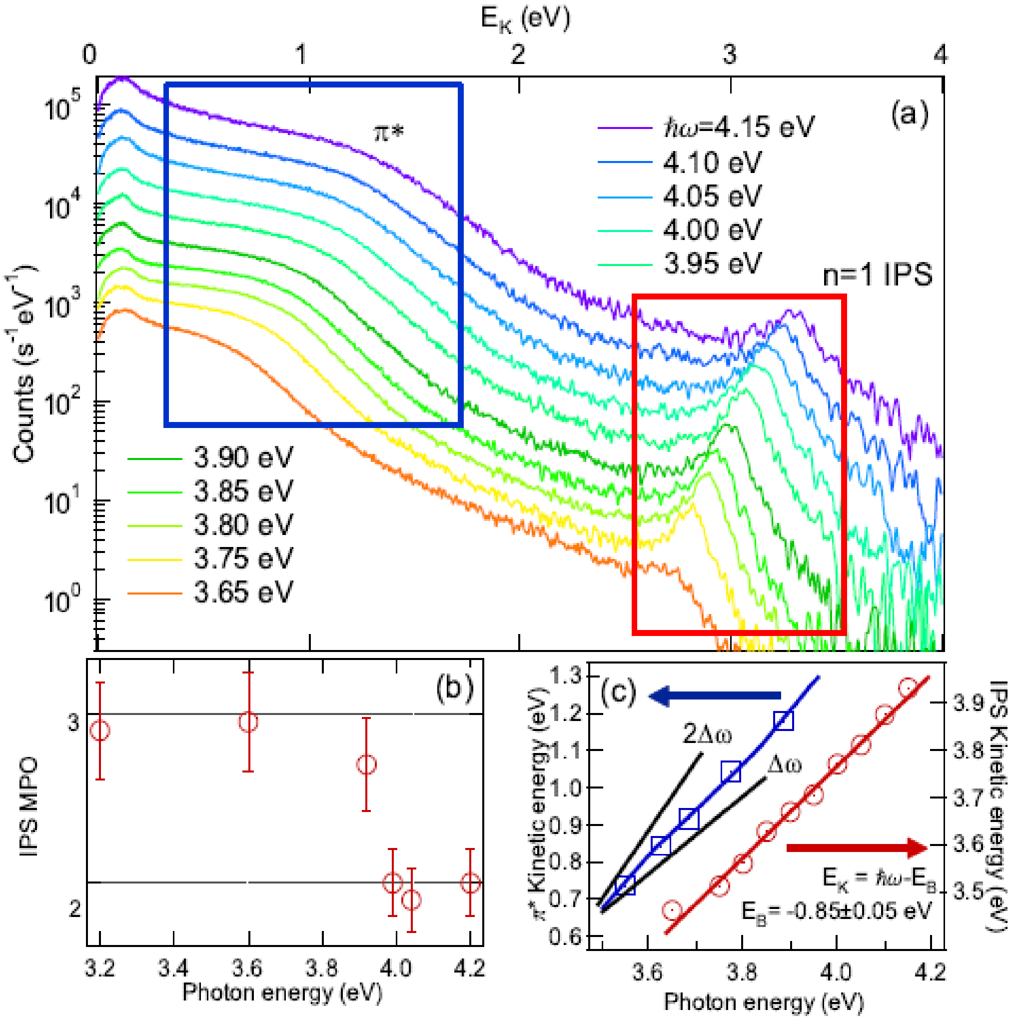

USING OPA – NOPA TO SPAN PHOTON ENERGY IN THE 3.2 – 4.2 RANGE

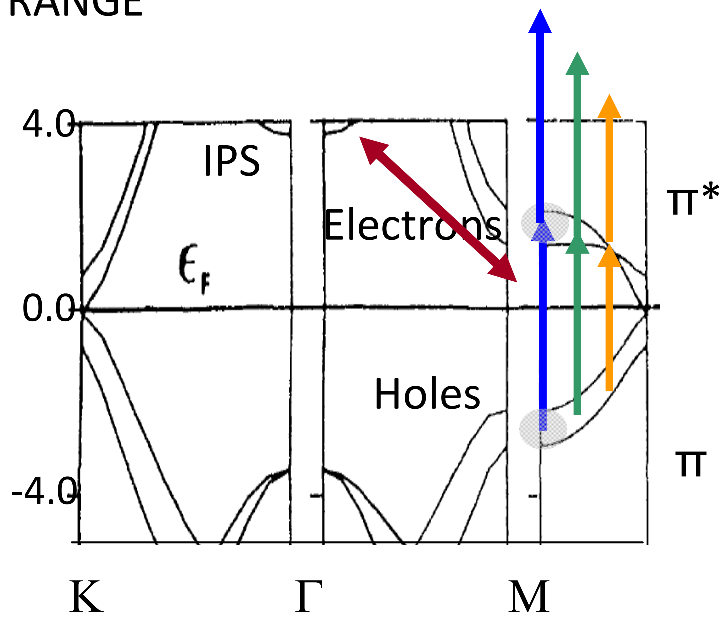

LINEAR IPS PHOTOEMISSION
RESONANT π → π* → vacuum

HOW ABOUT π* INTENSITY AND WIDTH?

IPS YIELD AND LINEWIDTH vs. ħω

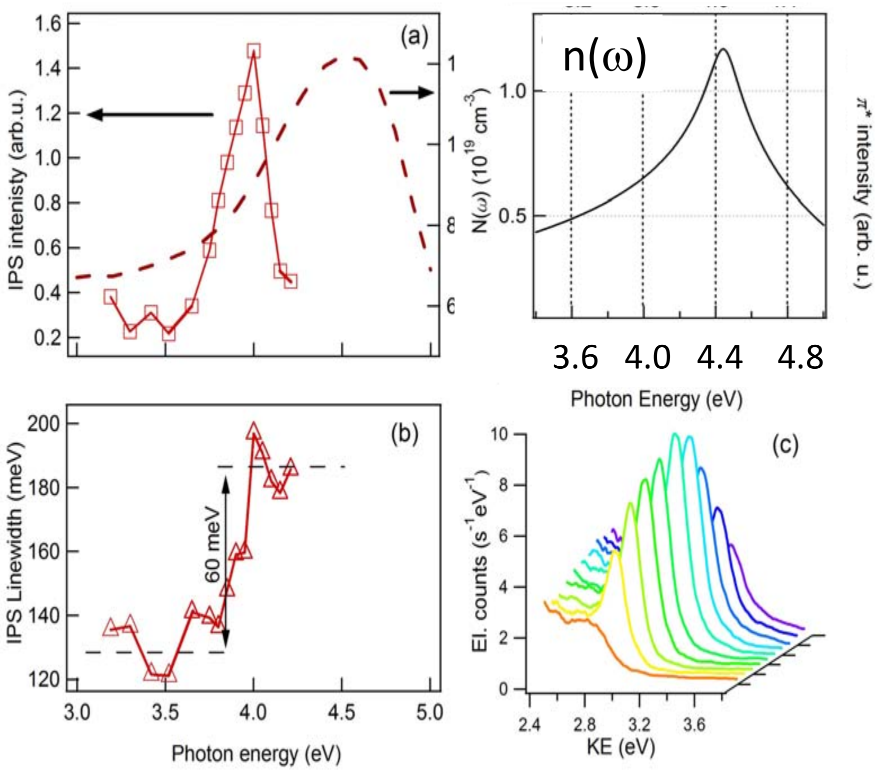

AT ħω=4.0 eV

PEAK IN THE IPS YIELD

STEP IN THE IPS FWHM of 60 meV

INTENSITY INCREASE : EXPLAINED BY OPTICAL ABSORPTION + MPO CHANGE

BUT:

0.4 eV SHIFT : BANDGAP RENORMALIZATION

IPS LINEWIDTH STEP: CHANGE IN LIFETIME?

HIGH IPS INTERACTION WITH BULK EXCITATIONS

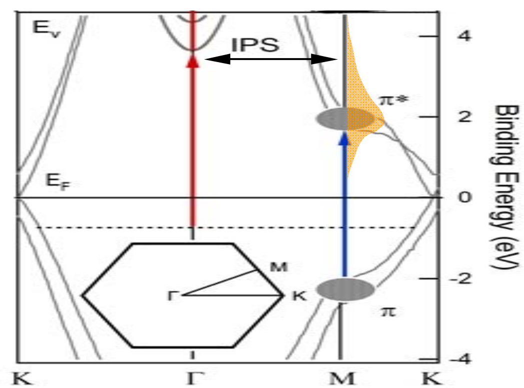

ANGLE RESOLVED SPECTRA: IPS EFFECTIVE MASS

C GEOMETRY

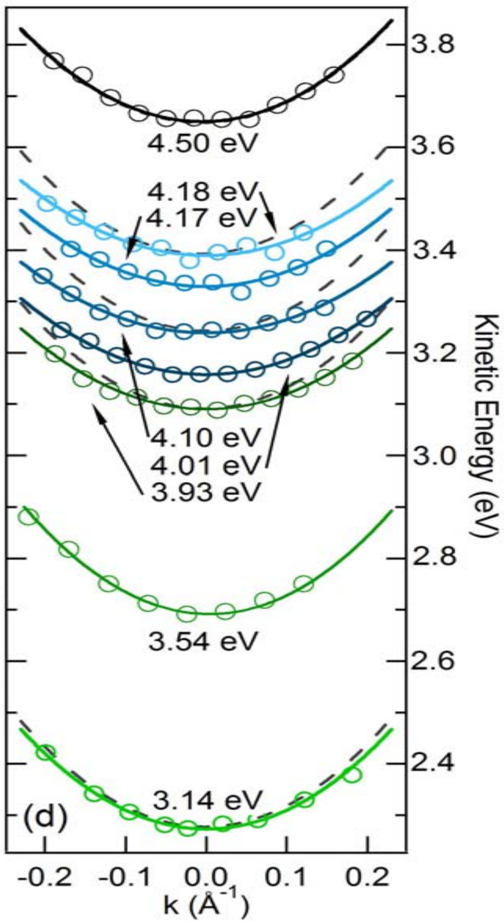

The IPS dispersion has been measured for the first time in HOPG

$$E_K(k_{\|}) = E_0 + \frac{\hbar^2 k_{\|}^2}{2m^*}$$

WE FOUND THAT m* DEPENDS on PHOTON ENERGY $\hbar\omega$

$\hbar\omega$ (eV)	3.14	3.54	3.93	4.01	4.10	4.17	4.18	4.50
$\langle m^* \rangle$	1.05	1.0	1.2	1.34	1.31	1.38	1.2	1.0

2DFEG

Maximum of m* @ 4.0 eV

IPS MASS RENORMALIZATION on HOPG

COULD BE INDUCED BY THE TRANSIENT OPTICAL EXCITATION in π BANDS

ROUGH, “SELF-ENERGY” APPROACH

ELECTRON POLARIZATION INTERACTION with IPS

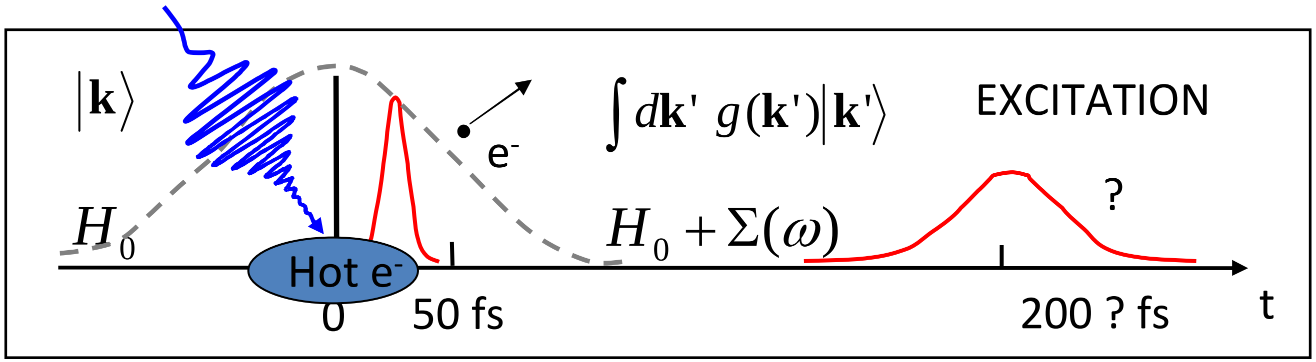

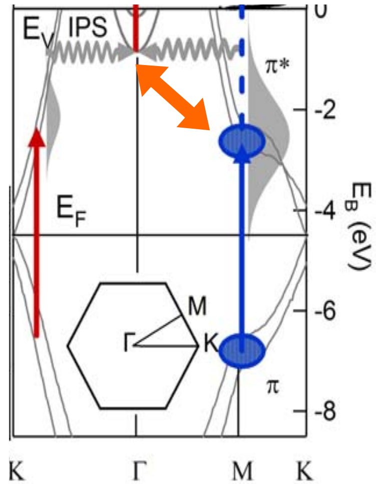

$$E_{\mathbf{k}} = E^0_{\mathbf{k}} + \mathrm{Re}\,\Sigma(\omega;\mathbf{k},E_{\mathbf{k}}/\hbar)$$

$$\gamma_{\mathbf{k}} = \mathrm{Im}\,\Sigma(\omega;\mathbf{k},E_{\mathbf{k}}/\hbar)$$

ANSATZ: $$\mathbf{Re}\,\Sigma(\omega) = \frac{n^2}{n_C^2}(\omega)\left(\alpha - \beta\frac{\hbar^2\mathbf{k}_{\parallel}^2}{2m}\right)$$

Primitive cell density FITTING PARAMETERS

$$n(\omega) = (1-R)\frac{F}{\hbar c}\epsilon_2(\omega - d\omega)$$

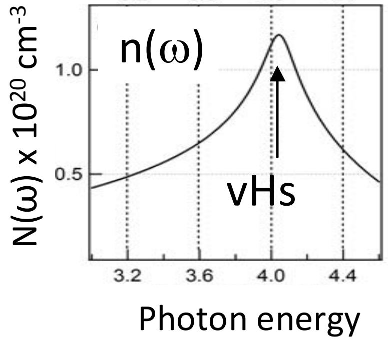

At k=0 USING KRAMERS-KRONIG RELATIONS:

$$\frac{m^*}{m_e}(\omega) = \frac{1}{1-\beta\,n^2(\omega)}$$

$$\mathbf{Im}\,\Sigma_\Gamma(\omega) = \alpha\,\mathbf{Im}\,\frac{2}{\pi}(\Gamma - i\omega)\int_0^\infty d\nu\,\frac{n^2(\nu)}{\nu^2 - (\omega + i\Gamma)^2}$$

FITTING RESULTS

Previous results allows us to fit C-geometry (symmetric) measurements without further analysis

IPS EFFECTIVE MASS

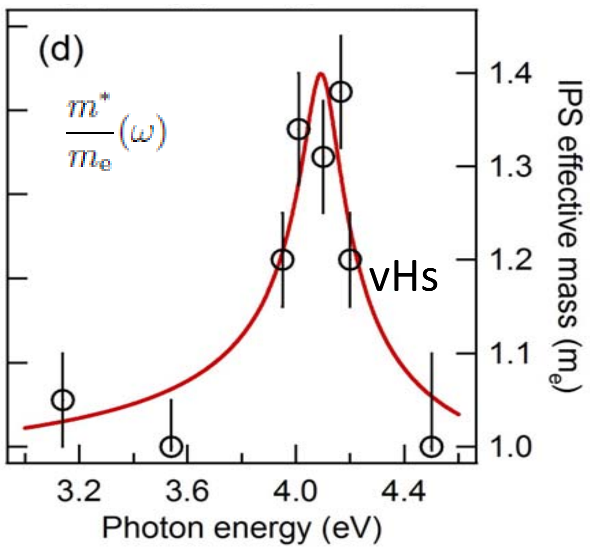

$$\frac{m^*}{m_e}(\omega) = \frac{1}{1 - \beta n^2(\omega)}$$

IPS FWHM

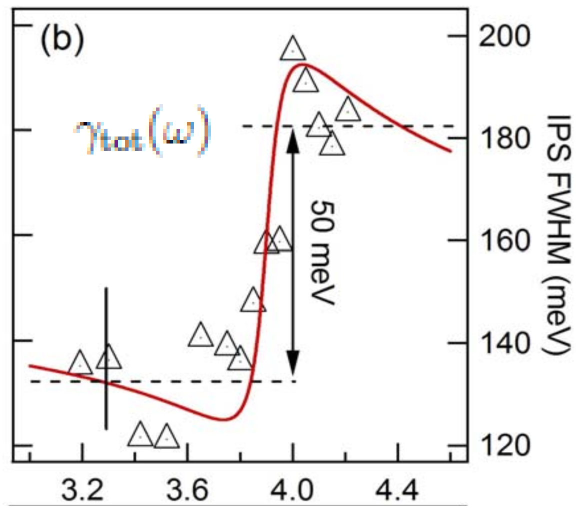

$$\mathrm{Im}\,\Sigma_\Gamma(\omega) = \alpha\,\mathrm{Im}\,\frac{2}{\pi}(\Gamma - i\omega)\int_0^\infty d\nu \frac{n^2(\nu)}{\nu^2 - (\omega + i\Gamma)^2}$$

PEAK / STEP IN CORRESPONDENCE OF THE RENORMALIZED VAN HOVE SINGULARITY

IPS effective mass AND linewidth behaviour are linked by the model.

Requests for TR-PES

-control of the photon density per pulse

-control of the rr (from 10 MHz to kHz regime)

-control of the polarization

-photon energy between 10 eV and ~10 keV

Future Light Sources 1

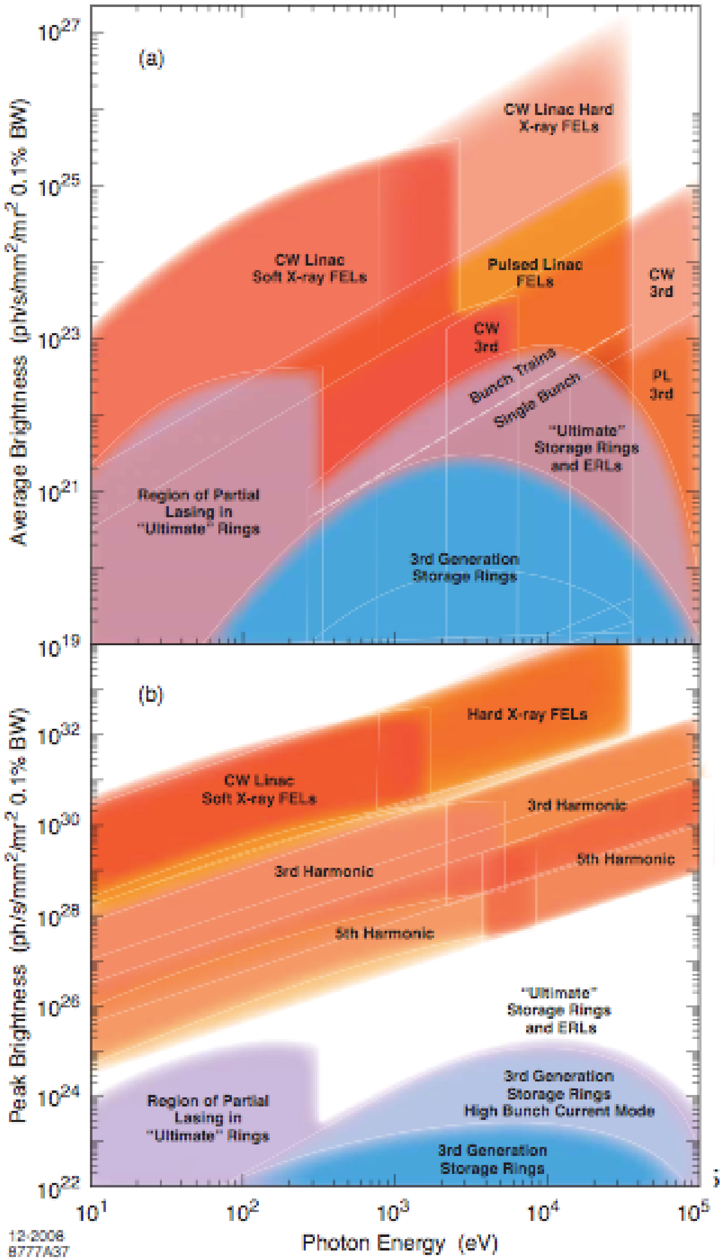

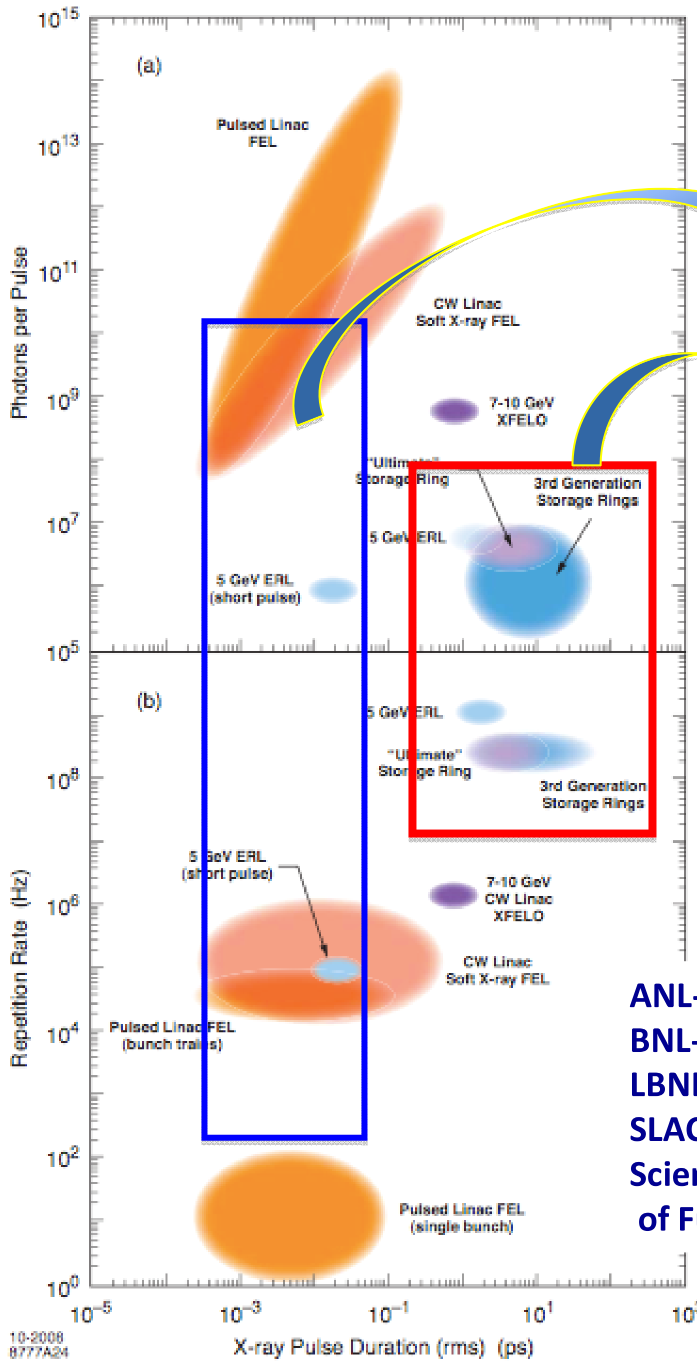

ANL-08/39
BNL-81895-2008
LBNL-1090E-2009
SLAC-R-917
Science and Technology of Future Light Sources

Future Light Sources 2

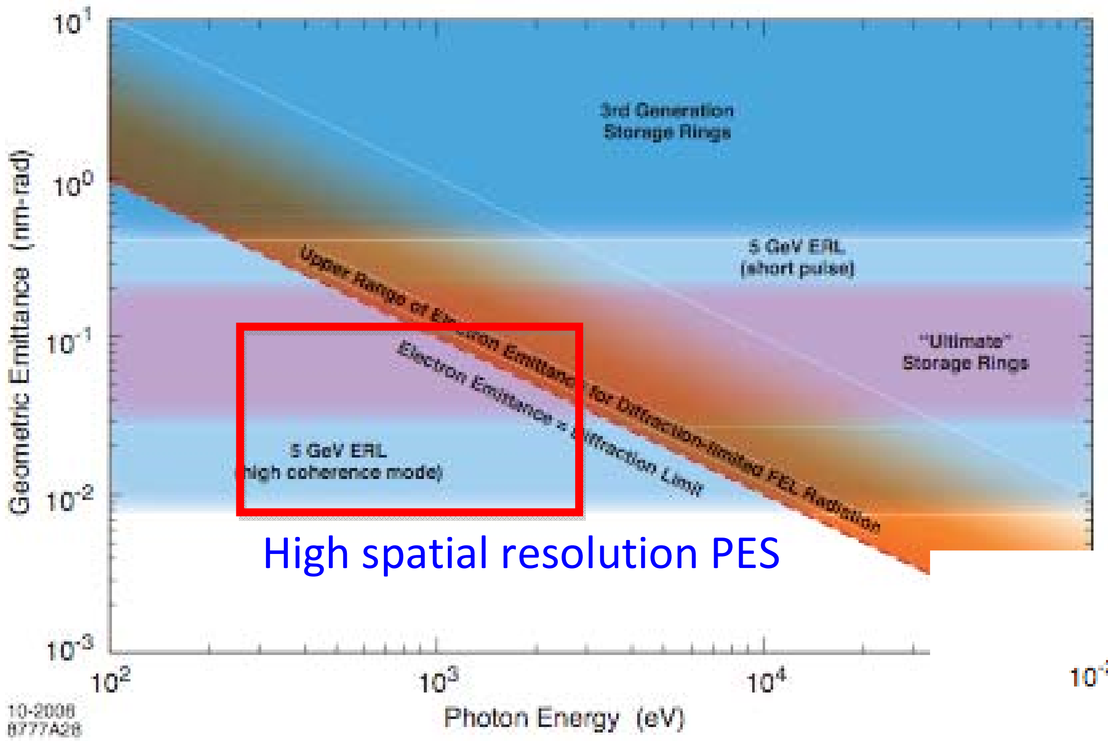

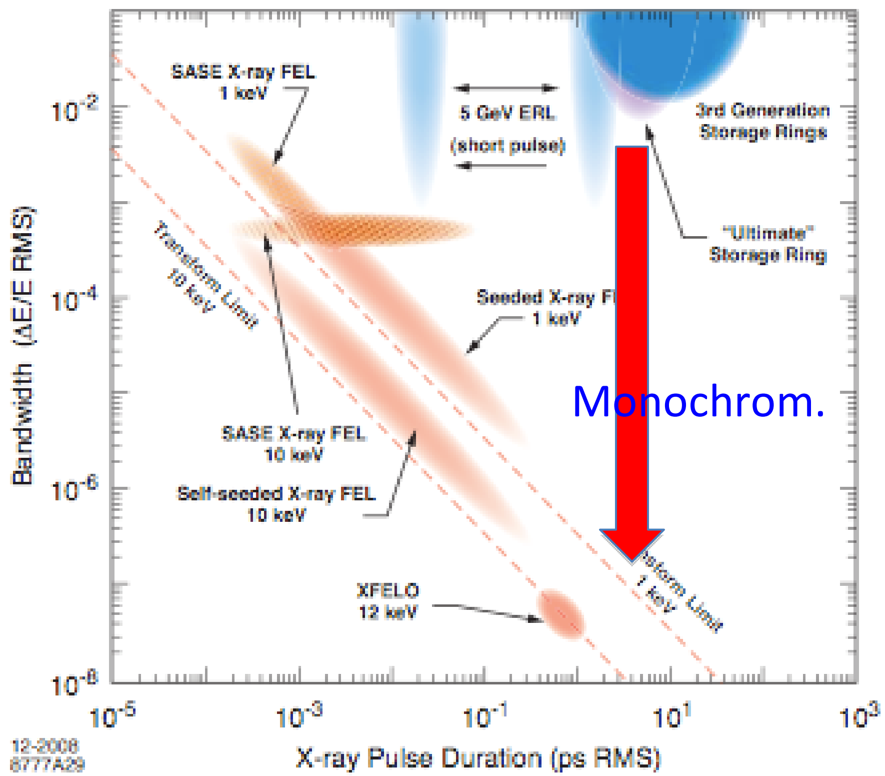

ANL-08/39
BNL-81895-2008
LBNL-1090E-2009
SLAC-R-917
Science and Technology of Future Light Sources

Conclusions

- **TR and SR PE-spectroscopy:**

1. Control of the photon density in the probing pulse
2. Selective pumping excitation
3. Controlled repetition rate (from kHz uo to MHz)
4. Photon energy range from few eV up to few keV
5. Very low temperature sample holder (6-degrees freedom)

- **Potential results:**

1. Dynamics of the Fermi surfaces
2. Electron-boson and electron-electron interactions in condensed matter (CDW, SDW and SC transition)
3. Electronic and magnetic structure of LDM
4. Dynamics of the VB and core elctrons

RESEARCH STAFF

Gabriele Ferrini

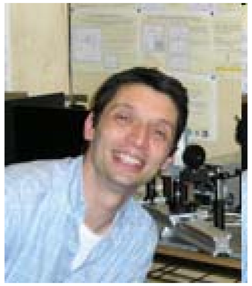

Gianluca Galimberti

Stefania Pagliara

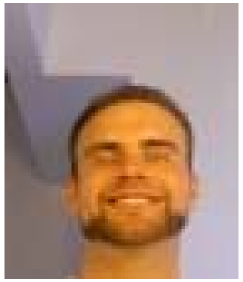

Matteo Montagnese

Stefano dal Conte

Cephise CACHO (ToF-POLARIMETER)

Barbara RESSEL (T-ReX)

Cesare Grazioli (T-ReX)

Michele ZACHIGNA (T-ReX)